are characteristics of alcoholic liver disease.[54] Thus, the reduction in serum folic acid observed in our rabbit NASH model might be a common feature of both alcoholic and nonalcoholic liver disease. Furthermore, the proteome analysis identified a reduction in GNMT and MAT1, which are associated with liver steatosis and fibrosis, in HFD II-fed rabbits.[55–57] Martínez-Chantar et al[55] showed that GNMT-knockout mice exhibited an elevation in serum aminotransferase, methionine, and *S*-adenosylmethionine and developed hepatic steatosis, fibrosis, and hepatocellular carcinoma. MAT1A-knockout mice were also reported to show liver steatosis.[57] These enzymes play an important role in the synthesis and degradation of *S*-adenosylmethionine.[56] Thus, an imbalance in *S*-adenosylmethionine and methionine metabolism may play a role in the development of steatohepatitis in our model.[58]

Phagocytic NADPH oxidases, such as gp91-phox, p40-phox, p67-phox, and p22-phox, increased in the present rabbit model (Supplemental Table S2, see *http://ajp.amjpathol.org*); however, the role of NADPH oxidase, a key molecule in the development of atherosclerosis,[59] in NASH is poorly understood. In alcoholic liver injury, NADPH oxidase is important for reactive oxygen species production in Kupffer cells and in hepatic stellate cells that initiate and promote liver injury.[60,61] We previously reported that the phagocytic activity of Kupffer cells promotes oxidative stress, inflammation, and fibrosis in steatohepatitis.[7] In this context, NADPH oxidase could play a prominent role in the pathogenesis of human NASH.

In the present study, we created a rabbit model of steatohepatitis, in which advanced fibrosis (close to cirrhosis) was produced by feeding a HFD. Hypercholesterolemia is a risk factor for liver injury as well as for atherosclerosis;[2–5] therefore, lowering the serum T-Cho level by dieting or by medications that reduce the synthesis and absorption of cholesterol could be a promising therapy for NAFLD including NASH. In this context, statins, which are HMG-CoA reductase inhibitors, have been reported to improve NASH.[62,63] Rallidis et al[62] showed that pravastatin treatment lowered serum ALT and improved histological steatosis in 5 NASH patients. Hyogo et al[63] treated patients with atorvastatin and found that 23 patients (74.2%) exhibited normalized transaminases and histological improvement of liver steatosis and the NAFLD activity score, and these changes were accompanied by a significant increase in serum adiponectin and a significant decrease in serum TNFα. In the present study, we studied the effect of ezetimibe, which inhibits NPC1L1 and therefore blocks intestinal absorption of cholesterol from the diet or that excreted in the bile.[11–15] The effect of ezetimibe on NASH has already been reported in rat models. Assy et al[19] studied methionine and choline deficiency-induced steatohepatitis in rats, in which ezetimibe administration alone or together with rosiglitazone, metformin, and valsartan reduced the hepatic levels of TG, T-Cho, and malondialdehyde and also significantly attenuated histological steatosis. In Zucker obese fatty rats, Deushi et al[18] reported that ezetimibe administration reduced the serum and hepatic levels of T-Cho and TG, the number of Oil red O-positive hepatocytes, Sirius red-stained collagen deposition, and αSMA expression. Supporting these observations, we demonstrated the usefulness of ezetimibe treatment in a rabbit NASH model. Because human lipid metabolism is similar to that of rabbits but is different from that of mice and rats, our results strengthen the potential of ezetimibe for controlling fat deposition and fibrosis in human NASH. Interestingly, ezetimibe not only improved HFD I-induced liver steatosis but also reduced fibrosis and the number of αSMA$^+$ cells. In chronic liver disease, TGFβ1 plays an important role in the progression of liver fibrosis and stellate cell activation.[43,44] TGFβ1 produced by Kupffer cells and stellate cells activates stellate cells in a paracrine as well as an autocrine manner and stimulates type I collagen production. In our rabbit model, ezetimibe reduced TGFβ1 and type I collagen expression in the liver. Unlike mice, humans and rabbits show abundant NPC1L1 expression in the liver.[15] Further studies are required to clarify the effect of ezetimibe prophylactically after the HFD-fed rabbits have already developed steatohepatitis and to examine whether ezetimibe directly affects cholesterol metabolism in hepatocytes, thereby participating in the local prevention of fibrosis caused by abnormal cholesterol metabolism.[14]

In conclusion, rabbits fed HFD II for 9 months developed steatohepatitis with advanced fibrosis accompanied by the augmented expression of relevant genes. We demonstrated the presence of an imbalance between oxidative stress and antioxidant levels in HFD II-fed rabbits. Ezetimibe therapy was promising for alleviating the pathological changes in this model, suggesting the potential usefulness of this compound for human liver diseases caused by cholesterol overload.

Acknowledgments

We thank Dr. Ryoko Shiga, Dr. Yong-ping Mu, Ms. Mami Mori, Ms. Michiko Ohashi, and Ms. Asuka Yoshida for their technical support.

References

1. Ford ES, Giles WH, Dietz WH: Prevalence of the metabolic syndrome among US adults: findings from the Third National Health and Nutrition Examination Survey. JAMA 2002, 287:356–359
2. Angulo P: Nonalcoholic fatty liver disease. N Engl J Med 2002, 346:1221–1231
3. Ludwig J, Viggiano TR, McGill DB, Oh BJ: Nonalcoholic steatohepatitis: Mayo Clinic experiences with a hitherto unnamed disease. Mayo Clin Proc 1980, 55:434–438
4. Matteoni CA, Younossi ZM, Gramlich T, Boparai N, Liu YC, McCullough AJ: Nonalcoholic fatty liver disease: a spectrum of clinical and pathological severity. Gastroenterology 1999, 116:1413–1419
5. Brunt EM, Janney CG, Di Bisceglie AM, Neuschwander-Tetri BA, Bacon BR: Nonalcoholic steatohepatitis: a proposal for grading and staging the histological lesions. Am J Gastroenterol 1999, 94:2467–2474
6. Neuschwander-Tetri BA, Caldwell SH: Nonalcoholic steatohepatitis: summary of an AASLD Single Topic Conference. Hepatology 2003, 37:1202–1219
7. Otogawa K, Kinoshita K, Fujii H, Sakabe M, Shiga R, Nakatani K, Ikeda K, Nakajima Y, Ikura Y, Ueda M, Arakawa T, Hato F, Kawada N: Erythrophagocytosis by liver macrophages (Kupffer cells) promotes oxidative stress, inflammation, and fibrosis in a rabbit model of

steatohepatitis: implications for the pathogenesis of human nonalcoholic steatohepatitis. Am J Pathol 2007, 170:967–980
8. Buja LM, Kita T, Goldstein JL, Watanabe Y, Brown MS: Cellular pathology of progressive atherosclerosis in the WHHL rabbit. An animal model of familial hypercholesterolemia. Arteriosclerosis 1983, 3:87–101
9. Okita M, Hayashi M, Sasagawa T, Takagi K, Suzuki K, Kinoyama S, Ito T, Yamada G: Effect of a moderately energy-restricted diet on obese patients with fatty liver. Nutrition 2001, 17:542–547
10. Huang MA, Greenson JK, Chao C, Anderson L, Peterman D, Jacobson J, Emick D, Lok AS, Conjeevaram HS: One-year intense nutritional counseling results in histological improvement in patients with non-alcoholic steatohepatitis: a pilot study. Am J Gastroenterol 2005, 100:1072–1081
11. Altmann SW, Davis HR Jr, Zhu LJ, Yao X, Hoos LM, Tetzloff G, Iyer SP, Maguire M, Golovko A, Zeng M, Wang L, Murgolo N, Graziano MP: Niemann-Pick C1 like 1 protein is critical for intestinal cholesterol absorption. Science 2004, 303:1201–1204
12. Davis HR Jr, Zhu LJ, Hoos LM, Tetzloff G, Maguire M, Liu J, Yao X, Iyer SP, Lam MH, Lund EG, Detmers PA, Graziano MP, Altmann SW: Niemann-Pick C1 like 1 (NPC1L1) is the intestinal phytosterol and cholesterol transporter and a key modulator of whole-body cholesterol homeostasis. J Biol Chem 2004, 279:33586–33592
13. Temel RE, Tang W, Ma Y, Rudel LL, Willingham MC, Ioannou YA, Davies JP, Nilsson LM, Yu L: Hepatic Niemann-Pick C1-like 1 regulates biliary cholesterol concentration and is a target of ezetimibe. J Clin Invest 2007, 117:1968–1978
14. Ge L, Wang J, Qi W, Miao HH, Cao J, Qu YX, Li BL, Song BL: The cholesterol absorption inhibitor ezetimibe acts by blocking the sterol-induced internalization of NPC1L1. Cell Metab 2008, 7:508–519
15. Hawes BE, O'Neill KA, Yao X, Crona JH, Davis HR Jr, Graziano MP, Altmann SW: In vivo responsiveness to ezetimibe correlates with Niemann-Pick C1 like-1 (NPC1L1) binding affinity: comparison of multiple species NPC1L1 orthologs. Mol Pharmacol 2007, 71:19–29
16. Knopp RH, Dujovne CA, Le Beaut A, Lipka LJ, Suresh R, Veltri EP: Evaluation of the efficacy, safety, and tolerability of ezetimibe in primary hypercholesterolaemia: a pooled analysis from two controlled phase III clinical studies. Int J Clin Pract 2003, 57:363–368
17. Gómez-Garre D, Munoz-Pacheco P, Gonzalez-Rubio ML, Aragoncillo P, Granados R, Fernandez-Cruz A: Ezetimibe reduces plaque inflammation in a rabbit model of atherosclerosis and inhibits monocyte migration in addition to its lipid-lowering effect. Br J Pharmacol 2009, 156:1218–1227
18. Deushi M, Nomura M, Kawakami A, Haraguchi M, Ito M, Okazaki M, Ishii H, Yoshida M: Ezetimibe improves liver steatosis and insulin resistance in obese rat model of metabolic syndrome. FEBS Lett 2007, 581:5664–5670
19. Assy N, Grozovski M, Bersudsky I, Szvalb S, Hussein O: Effect of insulin-sensitizing agents in combination with ezetimibe, and valsartan in rats with non-alcoholic fatty liver disease. World J Gastroenterol 2006, 12:4369–4376
20. Yamagishi S, Nakamura K, Matsui T, Sato T, Takeuchi M: Inhibition of intestinal cholesterol absorption by ezetimibe is a novel therapeutic target for fatty liver. Med Hypotheses 2006, 66:844–846
21. Buyssens N, Kockx MM, Herman AG, Lazou JM, Van den Berg K, Wisse E, Geerts A: Centrolobular liver fibrosis in the hypercholesterolemic rabbit. Hepatology 1996, 24:939–946
22. Seki S, Kitada T, Yamada T, Sakaguchi H, Nakatani K, Wakasa K: In situ detection of lipid peroxidation and oxidative DNA damage in non-alcoholic fatty liver diseases. J Hepatol 2002, 37:56–62
23. Otogawa K, Ogawa T, Shiga R, Nakatani K, Ikeda K, Nakajima Y, Kawada N: Attenuation of acute and chronic liver injury in rats by iron-deficient diet. Am J Physiol Regul Integr Comp Physiol 2008, 294:R311–R320
24. Kawada N, Kristensen DB, Asahina K, Nakatani K, Minamiyama Y, Seki S, Yoshizato K: Characterization of a stellate cell activation-associated protein (STAP) with peroxidase activity found in rat hepatic stellate cells. J Biol Chem 2001, 276:25318–25323
25. Kristensen DB, Kawada N, Imamura K, Miyamoto Y, Tateno C, Seki S, Kuroki T, Yoshizato K: Proteome analysis of rat hepatic stellate cells. Hepatology 2000, 32:268–277
26. Greco D, Kotronen A, Westerbacka J, Puig O, Arkkila P, Kiviluoto T, Laitinen S, Kolak M, Fisher RM, Hamsten A, Auvinen P, Yki-Jarvinen H: Gene expression in human NAFLD. Am J Physiol Gastrointest Liver Physiol 2008, 294:G1281–G1287
27. Nakamuta M, Kohjima M, Morizono S, Kotoh K, Yoshimoto T, Miyagi I, Enjoji M: Evaluation of fatty acid metabolism-related gene expression in nonalcoholic fatty liver disease. Int J Mol Med 2005, 16:631–635
28. Puri P, Baillie RA, Wiest MM, Mirshahi F, Choudhury J, Cheung O, Sargeant C, Contos MJ, Sanyal AJ: A lipidomic analysis of nonalcoholic fatty liver disease. Hepatology 2007, 46:1081–1090
29. Marí M, Caballero F, Colell A, Morales A, Caballeria J, Fernandez A, Enrich C, Fernandez-Checa JC, Garcia-Ruiz C: Mitochondrial free cholesterol loading sensitizes to TNF- and Fas-mediated steatohepatitis. Cell Metab 2006, 4:185–198
30. Begriche K, Igoudjil A, Pessayre D, Fromenty B: Mitochondrial dysfunction in NASH: causes, consequences and possible means to prevent it. Mitochondrion 2006, 6:1–28
31. Parola M, Robino G: Oxidative stress-related molecules and liver fibrosis. J Hepatol 2001, 35:297–306
32. Musso G, Gambino R, Durazzo M, Biroli G, Carello M, Faga E, Pacini G, De Michieli F, Rabbione L, Premoli A, Cassader M, Pagano G: Adipokines in NASH: postprandial lipid metabolism as a link between adiponectin and liver disease. Hepatology 2005, 42:1175–1183
33. Fu JF, Fang YL, Liang L, Wang CL, Hong F, Dong GP: A rabbit model of pediatric nonalcoholic steatohepatitis: the role of adiponectin. World J Gastroenterol 2009, 15:912–918
34. Sreekumar R, Rosado B, Rasmussen D, Charlton M: Hepatic gene expression in histologically progressive nonalcoholic steatohepatitis. Hepatology 2003, 38:244–251
35. Mofrad P, Contos MJ, Haque M, Sargeant C, Fisher RA, Luketic VA, Sterling RK, Shiffman ML, Stravitz RT, Sanyal AJ: Clinical and histologic spectrum of nonalcoholic fatty liver disease associated with normal ALT values. Hepatology 2003, 37:1286–1292
36. Wong VW, Wong GL, Tsang SW, Hui AY, Chan AW, Choi PC, Chim AM, Chu S, Chan FK, Sung JJ, Chan HL: Metabolic and histological features of non-alcoholic fatty liver disease patients with different serum alanine aminotransferase levels. Aliment Pharmacol Ther 2009, 29:387–396
37. Enomoto N, Yamashina S, Kono H, Schemmer P, Rivera CA, Enomoto A, Nishiura T, Nishimura T, Brenner DA, Thurman RG: Development of a new, simple rat model of early alcohol-induced liver injury based on sensitization of Kupffer cells. Hepatology 1999, 29:1680–1689
38. Tomita K, Tamiya G, Ando S, Ohsumi K, Chiyo T, Mizutani A, Kitamura N, Toda K, Kaneko T, Horie Y, Han JY, Kato S, Shimoda M, Oike Y, Tomizawa M, Makino S, Ohkura T, Saito H, Kumagai N, Nagata H, Ishii H, Hibi T: Tumour necrosis factor α signalling through activation of Kupffer cells plays an essential role in liver fibrosis of non-alcoholic steatohepatitis in mice. Gut 2006, 55:415–424
39. Wang HN, Wang YR, Liu GQ, Liu Z, Wu PX, Wei XL, Hong TP: Inhibition of hepatic interleukin-18 production by rosiglitazone in a rat model of nonalcoholic fatty liver disease. World J Gastroenterol 2008, 14:7240–7246
40. Szabo G, Velayudham A, Romics L Jr, Mandrekar P: Modulation of non-alcoholic steatohepatitis by pattern recognition receptors in mice: the role of Toll-like receptors 2 and 4. Alcohol Clin Exp Res 2005, 29:140S–145S
41. Rivera CA, Adegboyega P, van Rooijen N, Tagalicud A, Allman M, Wallace M: Toll-like receptor-4 signaling and Kupffer cells play pivotal roles in the pathogenesis of non-alcoholic steatohepatitis. J Hepatol 2007, 47:571–579
42. Akira S, Takeda K: Toll-like receptor signalling. Nat Rev Immunol 2004, 4:499–511
43. Kawada N: The hepatic perisinusoidal stellate cell. Histol Histopathol 1997, 12:1069–1080
44. Friedman SL: Molecular regulation of hepatic fibrosis, an integrated cellular response to tissue injury. J Biol Chem 2000, 275:2247–2250
45. Paik YH, Schwabe RF, Bataller R, Russo MP, Jobin C, Brenner DA: Toll-like receptor 4 mediates inflammatory signaling by bacterial lipopolysaccharide in human hepatic stellate cells. Hepatology 2003, 37:1043–1055
46. Seki E, De Minicis S, Osterreicher CH, Kluwe J, Osawa Y, Brenner DA, Schwabe RF: TLR4 enhances TGF-β signaling and hepatic fibrosis. Nat Med 2007, 13:1324–1332
47. Koruk M, Taysi S, Savas MC, Yilmaz O, Akcay F, Karakok M: Oxidative stress and enzymatic antioxidant status in patients with nonalcoholic steatohepatitis. Ann Clin Lab Sci 2004, 34:57–62
48. Nobili V, Pastore A, Gaeta LM, Tozzi G, Comparcola D, Sartorelli MR, Marcellini M, Bertini E, Piemonte F: Glutathione metabolism and an-

tioxidant enzymes in patients affected by nonalcoholic steatohepatitis. Clin Chim Acta 2005, 355:105–111
49. Yesilova Z, Yaman H, Oktenli C, Ozcan A, Uygun A, Cakir E, Sanisoglu SY, Erdil A, Ates Y, Aslan M, Musabak U, Erbil MK, Karaeren N, Dagalp K: Systemic markers of lipid peroxidation and antioxidants in patients with nonalcoholic fatty liver disease. Am J Gastroenterol 2005, 100:850–855
50. Chalasani N, Deeg MA, Crabb DW: Systemic levels of lipid peroxidation and its metabolic and dietary correlates in patients with nonalcoholic steatohepatitis. Am J Gastroenterol 2004, 99:1497–1502
51. Akin K, Beyler AR, Kaya M, Erden E: The importance of iron and copper accumulation in the pathogenesis of non-alcoholic steatohepatitis. Turk J Gastroenterol 2003, 14:228–233
52. Machado MV, Ravasco P, Jesus L, Marques-Vidal P, Oliveira CR, Proenca T, Baldeiras I, Camilo ME, Cortez-Pinto H: Blood oxidative stress markers in non-alcoholic steatohepatitis and how it correlates with diet. Scand J Gastroenterol 2008, 43:95–102
53. Wake K: "Sternzellen" in the liver: perisinusoidal cells with special reference to storage of vitamin A. Am J Anat 1971, 132:429–462
54. Purohit V, Abdelmalek MF, Barve S, Benevenga NJ, Halsted CH, Kaplowitz N, Kharbanda KK, Liu QY, Lu SC, McClain CJ, Swanson C, Zakhari S: Role of S-adenosylmethionine, folate, and betaine in the treatment of alcoholic liver disease: summary of a symposium. Am J Clin Nutr 2007, 86:14–24
55. Martínez-Chantar ML, Vazquez-Chantada M, Ariz U, Martinez N, Varela M, Luka Z, Capdevila A, Rodriguez J, Aransay AM, Matthiesen R, Yang H, Calvisi DF, Esteller M, Fraga M, Lu SC, Wagner C, Mato JM: Loss of the glycine N-methyltransferase gene leads to steatosis and hepatocellular carcinoma in mice. Hepatology 2008, 47:1191–1199
56. Wortham M, He L, Gyamfi M, Copple BL, Wan YJ: The transition from fatty liver to NASH associates with SAMe depletion in db/db mice fed a methionine choline-deficient diet. Dig Dis Sci 2008, 53:2761–2774
57. Lu SC, Alvarez L, Huang ZZ, Chen L, An W, Corrales FJ, Avila MA, Kanel G, Mato JM: Methionine adenosyltransferase 1A knockout mice are predisposed to liver injury and exhibit increased expression of genes involved in proliferation. Proc Natl Acad Sci USA 2001, 98:5560–5565
58. Mato JM, Lu SC: Role of S-adenosyl-L-methionine in liver health and injury. Hepatology 2007, 45:1306–1312
59. Park YM, Febbraio M, Silverstein RL: CD36 modulates migration of mouse and human macrophages in response to oxidized LDL and may contribute to macrophage trapping in the arterial intima. J Clin Invest 2009, 119:136–145
60. Bataller R, Schwabe RF, Choi YH, Yang L, Paik YH, Lindquist J, Qian T, Schoonhoven R, Hagedorn CH, Lemasters JJ, Brenner DA: NADPH oxidase signal transduces angiotensin II in hepatic stellate cells and is critical in hepatic fibrosis. J Clin Invest 2003, 112:1383–1394
61. Wheeler MD, Kono H, Yin M, Nakagami M, Uesugi T, Arteel GE, Gabele E, Rusyn I, Yamashina S, Froh M, Adachi Y, Iimuro Y, Bradford BU, Smutney OM, Connor HD, Mason RP, Goyert SM, Peters JM, Gonzalez FJ, Samulski RJ, Thurman RG: The role of Kupffer cell oxidant production in early ethanol-induced liver disease. Free Radic Biol Med 2001, 31:1544–1549
62. Rallidis LS, Drakoulis CK, Parasi AS: Pravastatin in patients with nonalcoholic steatohepatitis: results of a pilot study. Atherosclerosis 2004, 174:193–196
63. Hyogo H, Tazuma S, Arihiro K, Iwamoto K, Nabeshima Y, Inoue M, Ishitobi T, Nonaka M, Chayama K: Efficacy of atorvastatin for the treatment of nonalcoholic steatohepatitis with dyslipidemia. Metabolism 2008, 57:1711–1718

Laboratory Investigation (2010) 90, 245–256

Reversibility of fibrosis, inflammation, and endoplasmic reticulum stress in the liver of rats fed a methionine–choline-deficient diet

Yong-ping Mu[1,2], Tomohiro Ogawa[1] and Norifumi Kawada[1]

Fatty liver disease has become a health problem related to metabolic syndrome worldwide, although its molecular pathogenesis requires further study. It is also unclear whether advanced fibrosis of steatohepatitis will regress when diet is controlled. The aim of this study was to investigate whether the resolution of fibrosis occurs in steatohepatitis induced by a methionine–choline-deficient diet (MCDD). Manifestation of endoplasmic reticulum (ER) stress in this model was also studied. Nonalcoholic steatohepatitis with advanced fibrosis was induced in rats by feeding them an MCDD for 10 weeks. Instead of MCDD, a methionine–choline control diet (CD) was given for the last 2 weeks to the experimental group. Fibrosis and inflammation were determined by tissue staining. Protein and gene expressions were determined by immunoblotting and quantitative reverse transcription-PCR (RT-PCR), respectively. Expressions of caspase-7, caspase-12, glucose-regulated protein 78 (GRP78), and protein disulfide isomerase were evaluated to clarify the presence of ER stress. Changing the diet from MCDD to CD triggered the reduction of fat in hepatocytes, a decrease in inflammatory gene expression and oxidative stress, and regression of fibrosis accompanied by the disappearance of activated stellate cells and macrophages. Immunohistochemistry, immunoblotting, and RT-PCR analysis all indicated the occurrence of ER stress in steatohepatitis, while it recovered immediately after changing the diet from MCCD to CD. The ratio of hepatocyte proliferation/apoptotis increased significantly during the recovery stage. This simple experiment clearly shows that changing the diet from MCDD to a normal diet (CD) triggers the resolution of hepatic inflammatory and fibrotic reactions and hepatocyte apoptosis, suggesting that MCDD-induced steatohepatitis is also reversible. ER stress appears and disappears in association with the generation and regression of steatohepatitis, respectively, with fibrosis.
Laboratory Investigation (2010) **90,** 245–256; doi:10.1038/labinvest.2009.123; published online 30 November 2009

KEYWORDS: caspase; cytoglobin; hepatic stellate cells; hepatocytes; Kupffer cells; oxidative stress

Nonalcoholic fatty liver disease (NAFLD) is a relatively newly defined hepatic sequela of obesity and type II diabetes mellitus,[1–3] and it is one of the most common causes of chronic liver disease in many countries.[4] A number of studies have identified a significant correlation between hepatic steatosis and fibrosis.[5–7] NAFLD covers a progressive spectrum of liver pathologies from simple steatosis to nonalcoholic steatohepatitis (NASH), which is characterized by necroinflammation and fibrosis, and, subsequently, by cirrhosis.[8] It is also speculated that NASH may progress to hepatocellular carcinoma.[9–11]

Although adipocytokines, cytokines, and free fatty acids (FFAs) derived from peripheral and visceral fat tissues, which are known as mediators of metabolic syndrome, are assumed to contribute to the initiation of inflammatory reactions in the liver, the link between the development of hepatic steatosis and fibrosis is still poorly understood.[12] Furthermore, whether the regression of liver fibrosis caused by NASH occurs after controlling diet has not been proven, but the reversibility of liver fibrosis has been evidenced in patients who have successfully achieved the eradication of hepatitis C virus after interferon therapy.[13,14]

Over the past decade, it has become clear that obesity is associated with the activation of cellular stress signaling and inflammatory pathways.[15–17] A key cell organelle in cellular stress response is the endoplasmic reticulum (ER), a membranous network that functions in the synthesis and processing of secreted and membranous proteins. Certain

[1]Department of Hepatology, Graduate School of Medicine, Osaka City University, Osaka, Japan and [2]Shanghai Public Health Clinical Centre, Shanghai, China
Correspondence: Dr N Kawada, MD, PhD, Department of Hepatology, Osaka City University, Graduate School of Medicine, 1-4-3, Asahimachi, Abeno, Osaka 545-8585, Japan.
E-mail: kawadanori@med.osaka-cu.ac.jp

Received 26 March 2009; revised 2 September 2009; accepted 10 September 2009

pathological stress conditions disrupt ER homeostasis and lead to the accumulation of unfolded or misfolded proteins in the ER lumen, known as ER stress, resulting in the activation of signal transduction systems.[18–20] ER stress is caused by glucose or nutrient deprivation, viral infections, lipids, increased synthesis of secretory proteins, and expression of mutant or misfolded proteins, and has been recently implicated in human diseases, such as Alzheimer's disease, Parkinson's disease, diabetes mellitus, and liver disease.[21–24]

In this study, a rat steatohepatitis model induced by a methionine–choline-deficient diet (MCDD) for 10 weeks was used to obtain evidence for the resolution of fibrosis in fatty liver after changing the diet to a methionine–choline control diet (CD). The manifestation of ER stress was also studied. The results of this study clearly indicated that a dietary change from MCDD to CD immediately initiates tissue remodeling, which is associated with the cessation of cellular apoptosis and ER stress.

MATERIALS AND METHODS

Materials

Mouse monoclonal antibody against α-smooth muscle actin (α-SMA, Clone 1A4) and mouse monoclonal antibody against 5-bromo-2-deoxyuridine (BrdU, Clone 1BU33, 1:1000) were obtained from Sigma Chemical (St Louis, MO, USA). Rat monoclonal antibody against caspase-12 and goat polyclonal antibodies against glucose-regulated protein 78 (GRP78) were purchased from Santa Cruz Biotechnology (Santa Cruz, CA, USA). Rabbit polyclonal antibodies against caspase-7, rabbit polyclonal antibodies against cleaved caspase-7 (Asp198), and rabbit polyclonal antibodies against protein disulfide isomerase (PDI) were obtained from Cell Signaling Technology (Danvers, MA, USA). Mouse monoclonal antibody against CD68 (Clone, KP1) was purchased from Dako Denmark A/S (Glostrup, Denmark). Mouse monoclonal antibody against heme oxygenase-1 (HO-1, Hsp32) was obtained from Assay Designs (Ann Arbor, MI, USA). Mouse monoclonal antibody against 4-hydroxy-2-nonenal (4-HNE) was purchased from the Japan Institute for the Control of Aging (Shizuoka, Japan). Mouse monoclonal antibody against glyceraldehyde-3-phosphate dehydrogenase (GAPDH) was obtained from Chemicon International (Temecula, CA, USA). Rabbit anti-cytoglobin antibodies were produced in our laboratory as described previously.[25] Horseradish peroxidase (HRP)-conjugated polyclonal rabbit anti-goat immunoglobulins, HRP-conjugated polyclonal rabbit anti-mouse immunoglobulins, HRP-conjugated polyclonal rabbit anti-rat immunoglobulins, and HRP-conjugated polyclonal swine anti-rabbit immunoglobulins were obtained from Dako Denmark A/S. Hybond-ECL nitrocellulose membranes and ECL detection reagent were obtained from Amersham Pharmacia Biotech (Buckinghamshire, UK). All other reagents were purchased from Sigma Chemical or Wako Pure Chemical.

Animals and Experimental Protocol

Pathogen-free male Wistar rats (7–8 weeks of age) were obtained from SLC (Shizuoka, Japan). Animals were housed at a constant temperature and supplied with laboratory chow and water *ad libitum*. The experimental protocol was approved by the Animal Research Committee of Osaka City University (Guide for Animal Experiments, Osaka City University).

The rats were fed a CD (group C, $n=5$) or MCDD (group M, $n=5$) for 10 weeks. The contents of MCDD and CD are listed in Supplementary Table 1. A recovery model (group R, $n=5$) was produced by administering MCDD for 8 weeks and thereafter CD for 2 weeks. During the experimental period, individual body weights were recorded twice per week (see Supplementary Table 2).

Sample Harvesting

At the end of the tenth week, rats were killed under ether anesthesia, and the portal vein was cannulated using an 18-G Teflon catheter. Blood samples were collected from the inferior vena cava, centrifuged at 3000 r.p.m. for 30 min at 4°C, and the obtained sera were kept at −70°C until further use for serum chemistry tests. The liver of each animal was perfused with 100 ml of phosphate-buffered saline (pH 7.0) to remove blood and then washed with ice-cold saline, dried using filter paper, and weighed in a wet state. A portion of the liver was fixed with 4% paraformaldehyde, embedded in paraffin, and frozen. Another portion of the liver was snap-frozen in liquid nitrogen and stored at −70°C until use for reverse transcription-PCR (RT-PCR) and immunoblots.

Serum Chemistries

Serum levels of alanine aminotransferase (ALT), aspartate aminotransferase (AST), triglycerides (TGs), and FFAs were measured at Special Reference Laboratories (Osaka, Japan).

Histochemical and Immunohistochemical Analyses of the Rat Liver

Paraformaldehyde-fixed specimens were cut into 5-μm-thick sections and stained for 1 h with 0.1% (w/v) Sirius Red (Direct Red 80; Aldrich, Milwaukee, WI, USA), Oil red O, or hematoxylin and eosin (H&E). Immunohistochemistry was performed according to the methods described elsewhere.[26] Briefly, sections were deparaffinized, washed, and pre-incubated in blocking solution, followed by incubation with anti-4-HNE (15 μg/ml), HO-1 (1:50), CD68 (1:100), α-SMA (1:100), cytoglobin (1:400), or caspase-12 (1:100) antibodies. Sections were then incubated with HRP-conjugated secondary antibodies (1:1000), washed, covered with DAB, and counterstained with hematoxylin. Some of the immunostainings were performed at the Biopathology Institute (Oita, Japan). The red area on Oil red O staining was image analyzed by LuminaVision (Mitani Corporation, Tokyo, Japan).

TdT-Mediated dUTP Nick-End Labeling Assays

For the detection of apoptotic cells, paraffin-embedded sections were stained with the TdT-Mediated dUTP Nick-End Labeling (TUNEL) technique using an *In Situ* Apoptosis Detection kit (Takara Shuzo, Ohtsu, Japan) according to the manufacturer's instructions. For semi-quantitative analysis, the number of TUNEL-positive cells was counted in five randomly selected fields by viewing each slide at a magnification of × 400, and the average number in each group was calculated, as described previously.[27]

BrdU Assay for Hepatocyte Proliferation

For the detection of hepatocyte proliferation, rats were i.p. injected with BrdU (100 μg/kg) 2 h before being killed. *In situ* detection of the incorporation of BrdU into the nuclei was conducted immunohistochemically.[28] For semi-quantitative analysis, as for TUNEL, the number of BrdU-positive cells was counted in five randomly selected fields by viewing each slide at a magnification of × 200, and the average number in each group was calculated.

Quantitative RT-PCR

mRNA expressions of tumor necrosis factor-alpha (TNF-α), transforming growth factor-beta 1 (TGF-β1), α-SMA, collagen 1A2 (COL1A2), matrix metalloproteinases (MMPs)-2, -9, and -13, tissue inhibitor of MMP-1 (TIMP-1), caspases-3, -7, -9, and -12, GRP78, interleukin-6 (IL-6), BAX, BAK, Bcl-xl, Bcl-2, and ERp57 were assessed by quantitative RT-PCR. Total RNA was extracted from liver tissues using Isogen (Nippon Gene, Tokyo, Japan).[29] The expression of mRNA was measured using TaqMan One-Step RT-PCR Master Mix Reagents (Applied Biosystems, Foster City, CA, USA) or using the One-Step SYBR RT-PCR Kit (Perfect Real Time; Takara Bio, Ohtsu, Japan), and Applied Biosystems Prism 7700 (Applied Biosystems) according to a previously reported procedure.[27] Primers and oligonucleotide probes were designed using Primer Express (Sigma Chemical), and are listed in Table 1. Each PCR amplification was performed on five rats in both experimental and control groups. Individual gene expression was normalized by GAPDH. The conditions for the TaqMan One-Step RT-PCR were as follows: 30 min at 48°C (stage 1, RT), 10 min at 95°C (stage 2, RT inactivation and Ampli Taq Gold activation), and then 40 cycles of amplification for 15 s at 95°C and 1 min at 60°C (stage 3, PCR). The conditions for the One-Step SYBR RT-PCR (Perfect Real Time) were as follows: an initial step of 15 min at 42°C, 2 min at 95°C, and then 40 amplification cycles of denaturation at 95°C for 15 s, and annealing and extension at 60°C for 1 min.

Immunoblot Analysis

Some protein levels were assessed by immunoblot analysis, as described previously.[29] The liver tissue was lysed by RIPA buffer containing 50 mM Tris-HCl (pH 7.2), 150 mM NaCl, 1% NP-40, 0.1% SDS, 1 mM EDTA, and 1 mM PMSF and then homogenized in ice-cold water. After centrifugation for 10 min at 4°C and 12 000 r.p.m., the protein concentration of the obtained supernatant was determined using the Bio-Rad Dc protein Assay Reagent (Bio-Rad, Hercules, CA, USA). Protein was electrophoretically resolved in 10 or 12% SDS polyacrylamide gel, and successively transferred to Hybond-ECL nitrocellulose membranes. The membranes were blocked by 5% non-fat dietary milk solution in Tris-buffered saline (20 mM Tris and 150 mM NaCl, pH 7.4) with 0.1% Tween-20. They were then incubated overnight with primary antibodies at 4°C and successively with secondary antibodies at room temperature for 1 h. The following dilutions of primary antibodies were used: mouse monoclonal antibody to α-SMA, 1:1000; rabbit polyclonal antibodies to cytoglobin, 1:200; rat monoclonal antibody to caspase-12, 1:200; goat polyclonal antibodies to GRP78, 1:200; rabbit polyclonal antibodies to caspase-7, 1:1000; rabbit polyclonal antibodies to cleaved caspase-7 (Asp198), 1:1000; rabbit polyclonal antibodies against PDI, 1:200; mouse monoclonal antibody to GAPDH, 1:30 000. Immune complexes were visualized using a SuperSignal West Pico Chemiluminescent Substrate (ECL, Pierce, Rockford, IL, USA). Finally, band intensity was determined by scanning video densitometry.

Statistical Analysis

All results are expressed as mean ± s.d. Statistical analysis was performed using Student's *t*-test ($P<0.05$ was considered significant).

RESULTS

Accumulation of Fat in the Liver and Recovery after Dietary Change

As shown in Figure 1a and b, Oil red O staining clearly indicated that the MCDD diet (group M) for 10 weeks induced fat accumulation in the liver, especially in hepatocytes. It was also recognized that fat accumulation immediately decreased in group R ($P<0.01$), whose diet was changed from MCDD to CD during the last 2 weeks. The serum level of FFA was reduced in group M (183 ± 31.6 μequiv./l) compared with control group C (274 ± 35.7 μequiv./l) and recovery group R (267 ± 36.5 μequiv./l) ($P<0.01$). Similarly, the serum level of TG was reduced in group M (4.33 ± 1.21 mg/dl) compared with control group C (23.5 ± 4.95 mg/dl) and group R (28.2 ± 4.97 mg/dl) ($P<0.01$) (Figure 1c and d, $P<0.01$). Changes in the body weights of rats in each group are presented in Supplementary Table 2.

Liver Histology and Kupffer Cell Activation

H&E staining showed that the livers in group C showed an intact tissue structure, whereas those in group M showed the apparent vacuolization of hepatocytes, focal necrosis, and inflammatory cell accumulation in the parenchyma. These pathological changes were clearly improved in group R (Figure 2a). In accordance with this histological recovery, serum levels of AST and ALT were reduced from 97.7 ± 13.5

Table 1 Primer pairs and probes used for real-time PCR

Primer name	*Sequence*	*Note*
TNF-α		TaqMan
Forward	5′-GCT CCC TCT CAT CAG TTC CAT G-3′	
Reverse	5′-TAC GGG CTT GTC ACT CGA GTT TTG-3′	
Probe	5′-CCC AGA CCC TCA CAC TCA GAT CAT CTT C-3′	
Heme oxygenase-1		SYBR Green
Forward	5′-CGT GGC AGT GGG AAT TTA TG-3′	
Reverse	5′-AGG CTA CAT GAG ACA GAG TTC ACA-3′	
TGF-β1		TaqMan
Forward	5′-TGC TTC CGC ATC ACC GT-3′	
Reverse	5′-TAG TAG ACG ATG GGC AGT GGC-3′	
Probe	5′-CTG CGT GCC GCA GGC TTT GG-3′	
Collagen IA2		TaqMan
Forward	5′-AAG GGT CCT TCT GGA GAA CC-3′	
Reverse	5′-TCG AGA GCC AGG GAG ACC CA-3′	
Probe	5′-CAG GGT CTT CTT GGT GCT CCC GGT AT-3′	
α-SMA		TaqMan
Forward	5′-GAG GAG CAT CCG ACC TTGC-3′	
Reverse	5′-TTT CTC CCG GTT GGC CTTA-3′	
Probe	5′-AAC GGA GGC GCC GCT GAA CC-3′	
MMP-2		TaqMan
Forward	5′-CCG AGG ACT ATG ACC GGG ATA A-3′	
Reverse	5′-CTT GTT GCC CAG GAA AGT GAA G-3′	
Probe	5′-TCT GCC CCG AGA CCG CTA TGT CCA-3′	
MMP-9		SYBR Green
Forward	5′-GAC AAT CCT TGC AAT GTG GAT G-3′	
Reverse	5′-CCG ACC GTC CTT GAA GAA ATG-3′	
MMP-13		SYBR Green
Forward	5′-TGA CCT GGG ATT TCC AAA AGA G-3′	
Reverse	5′-TCT TCC CCG TGT CCT CAA A-3′	
TIMP-1		SYBR Green
Forward	5′-TCA GCC ATC CCT TGC AAA-3′	
Reverse	5′-GAG CCC ATG AGG ATC TGA TCT-3′	

Table 1 Continued

Primer name	*Sequence*	*Note*
Caspase-12		SYBR Green
Forward	5′-GGC AGA CAT ACT GGT ACT ATT TGG G-3′	
Reverse	5′-GCT CAA CAC ACA TTC CTC ATC TGT-3′	
Caspase-9		SYBR Green
Forward	5′-TGG ACA TTG GTT CTG GCA GAG-3′	
Reverse	5′-GTG TAT GCC ATA TCT GCA TGT CTC-3′	
Caspase-7		SYBR Green
Forward	5′-TAC AAG ATC CCG GTG GAA GCT-3′	
Reverse	5′-CTG GGT TCC TCC ACG AAT AAT AG-3′	
Caspase-3		SYBR Green
Forward	5′-AGA AAT TCA AGG GAC GGG TC-3′	
Reverse	5′-TGC GCG TAC AGT TTC AGC A-3′	
GRP78		SYBR Green
Forward	5′-CCA TCA CCA ATG ACC AAA ACC-3′	
Reverse	5′-GCG CTC TTT GAG CTT TTT GTC T-3′	
ERp57		SYBR Green
Forward	5′-TGAATGCTGAAGACAAGGACGTG-3′	
Reverse	5′-CATTGGCTGTGGCATCCATC-3′	
BAX		SYBR Green
Forward	5′-TAAAGTGCCCGAGCTGATCAGAACC-3′	
Reverse	5′-CCTGGTCTTGGATCCAGACAAGCA-3′	
BAK		SYBR Green
Forward	5′-GAGTTTGCGTAGAGACCCCATCCT-3′	
Reverse	5′-CCACAAATTGGCCCAACAGAACCA-3′	
Bcl-xl		SYBR Green
Forward	5′-TGCGTGGAAAGCGTAGACAAGGA-3′	
Reverse	5′-AAGGCTCTAGGTGGTCATTCAGGT-3′	

Table 1 Continued

Primer name	*Sequence*	*Note*
Bcl-2		SYBR Green
Forward	5′-TCGCGACTTTGCAGAGATGTCC-3′	
Reverse	5′-ACCCCATCCCTGAAGAGTTCCT-3′	
IL-6		
Forward	5′-TGT CTC GAG CCC ACC AGG-3′	TaqMan
Reverse	5′-TGC GGA GAG AAA CTT CAT AGC TG-3′	
Probe	5′-CGA AAG TCA ACT CCA TCT GCC CTT CAG G-3′	
STAT3		
Forward	5′-CAA TAC CAT TGA CCT GCC GAT-3′	SYBR Green
Reverse	5′-CCC CGT TAT TTC CAA ACT GC-3′	
GAPDH		TaqMan
Forward	5′-AAG ATG GTG AAG GTC GGT GTG-3′	
Reverse	5′-GAA GGC AGC CCT GGT AACC-3′	
Probe	5′-CGG ATT TGG CCG TAT CGG ACGC-3′	
GAPDH		SYBR Green
Forward	5′-AAT GCA TCC TGC ACC ACC AAC TGC-3′	
Reverse	5′-GGA GGC CAT GTA GGC CATG AGG TC-3′	

and 98.5 ± 14.9 IU/ml in group M and from 51.2 ± 13.8 and 35.4 ± 3.3 IU/ml in group R, respectively ($P<0.01$). Cells positive for CD68, a marker of activated Kupffer cells, increased in number (Figure 2b) in group M. The expression of TNF-α mRNA, which is known to be derived from activated Kupffer cells in the liver, increased to 2.5-fold in group M (Figure 2e, $P<0.01$) compared with group C, and returned to the normal range in group R ($P<0.01$). These results indicate that the change in diet from MCDD to CD reduced inflammatory reactions, Kupffer cell activation, and AST/ALT release from hepatocytes.

Oxidative Stress and its Recovery in Steatohepatitis

We used the immunostaining of 4-HNE to detect the production of oxidative aldehyde by lipid peroxidation in the liver. As shown in Figure 3a, the control liver of group C exhibited negligible staining by anti-4-HNE antibodies. In contrast, the liver in group M showed brown-colored hepatocytes and stained cells also accumulated at necrotic foci (magnified area). The number of 4-HNE-positive cells and the amount of granulomatous accumulation in cells, presumably macrophages, were clearly reduced in group R.

These results were reproduced on immunostaining of HO-1. As shown in Figure 3b, HO-1 expression is restricted in hepatic sinusoids, presumably in Kupffer cells (magnified area). However, in group M, HO-1-positive cells additionally led to an aggregation of cells next to vacuolized hepatocytes (magnified area). These reactions immediately disappeared in group R. In accordance with these results, HO-1 mRNA expression determined by RT-PCR was significantly augmented in group M compared with group C (5.19 ± 1.08 *vs* 3.13 ± 0.26, respectively, $P<0.01$) and returned to the normal level in group R.

Taken together, it can be stated that the accumulation of Oil red O-stained lipids, 4-HNE, and CD68- and HO-1-positive macrophages by administering an MCDD diet generates oxidative stress and hepatocyte damage (increase in AST and ALT levels), resulting in inflammatory gene expression, such as TNF-α. However, switching the diet from MCDD to CD immediately triggers the inhibition of inflammatory reactions.

Regression of Fibrosis and Hepatic Stellate Cell Activation in Steatohepatitis

Sirius Red staining (Figure 4a) clearly revealed collagen deposition with C-C and P-C bridges, near to cirrhosis, in the fibrotic septum of group M, although collagen deposition was observed only around veins in the intact liver (group C). An immediate and marked recovery of this advanced fibrosis was observed in group R, indicating that the change in diet from MCDD to CD triggers the regression of fibrosis in the liver within 2 weeks.

Immunohistochemistry of α-SMA and cytoglobin, markers of activated stellate cells and liver myofibroblasts, showed that hepatic fibrotic cell activation occurred in group M, whereas the process ceased immediately in group R (Figure 4b and c). Immunoblot analyses confirmed these immunohistochemical observations (Figure 4d). Furthermore, as shown in Figure 4e, RT-PCR analyses indicated that mRNA expressions of all α-SMA, TGF-β1, Col1A2, TIMP-1, MMP-2, and MMP-9 increased significantly in group M, and thereafter returned to the original level in group R. Conversely, the expression of MMP-13 decreased significantly in group M (0.98 ± 0.30 *vs* 3.39 ± 1.24, $P<0.01$) and recovered significantly in group R (2.30 ± 1.11). Thus, the recovery of fibrosis is evident at levels of histology, fibrotic protein, and fibrotic gene expression after switching the diet from MCDD to CD.

The Change of Hepatocyte Apoptosis and Proliferation

TUNEL staining showed that the number of apoptotic hepatocytes slightly increased in group M compared with group C (68.2 ± 15.9 *vs* 40.3 ± 8.33 cells per field, respectively, $P<0.05$), whereas it decreased significantly in group R (48.0 ± 6.48 cells per field) (Figure 5a and c).

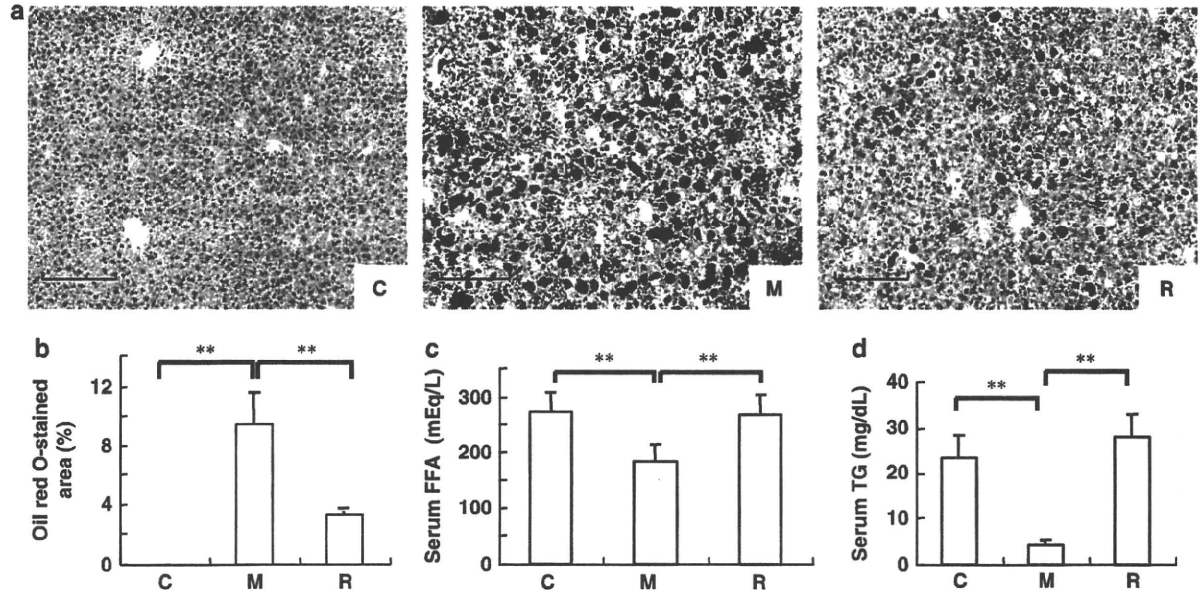

Figure 1 Oil red O staining in the liver and the serum level of FFA and TG. (**a**) Oil red O staining (× 200). Five sections per group were measured. Bar, 25 μm. (**b**) Percentage of Oil red O-stained area was determined using an image analyzer (LuminaVision). Group C, 0%; group M, 9.45% ($P<0.01$ compared with group C); group R, 3.27% ($P<0.01$ compared with group M). (**c**) Serum level of FFA (μequiv./l). $^{**}P<0.01$. (**d**) Serum level of TG (mg/dl). $^{**}P<0.01$.

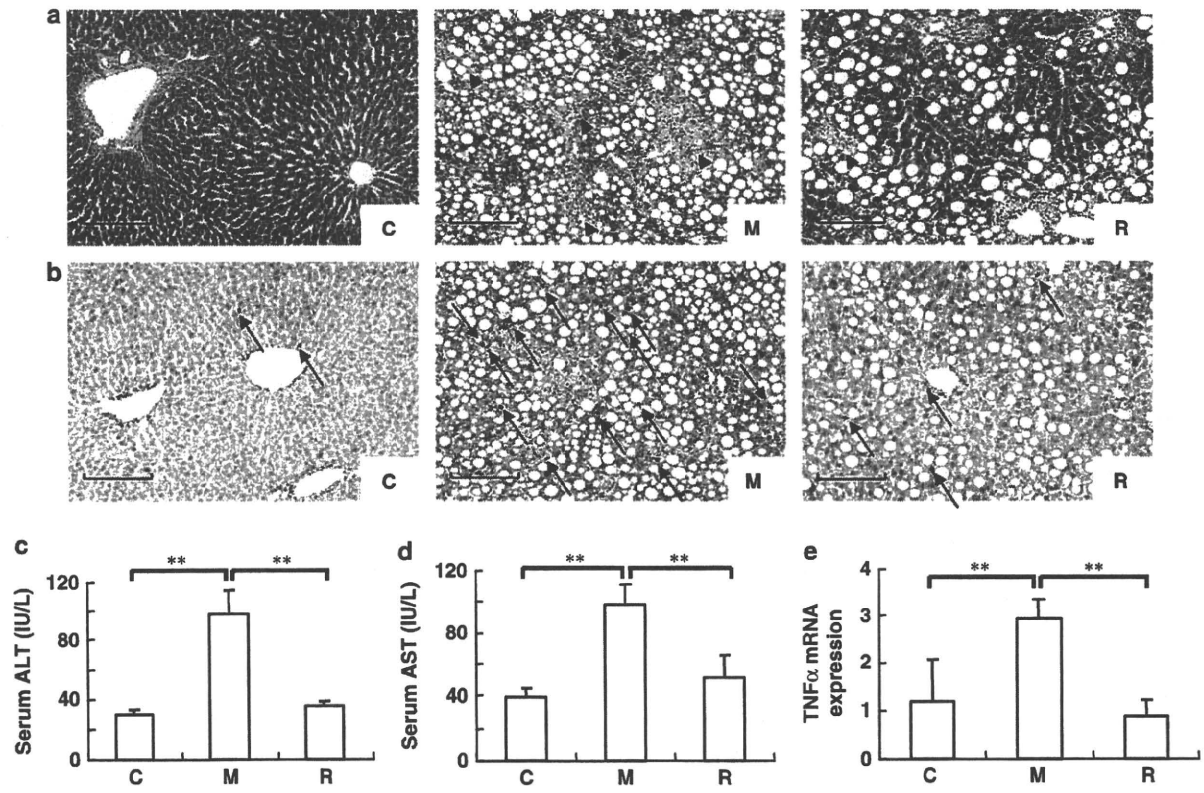

Figure 2 Kupffer cell activation and inflammation. (**a**) H&E staining (× 200). In group M, hepatocytes with fatty degeneration and inflammatory cell foci (arrowheads) were distributed in the parenchyma, whereas their number decreased in group R. Bar, 25 μm. (**b**) CD68 immunostaining (arrows) (× 200). CD68, a macrophage marker and low-density lipoprotein binding site, was rare in group C, whereas CD68-positive cells increased in number in group M, and decreased in group R. Bar, 25 μm. (**c** and **d**) Serum levels of ALT and AST. (**e**) The relative TNF-α mRNA level measured by RT-PCR. The TNF-α mRNA level was normalized by the GAPDH mRNA level.

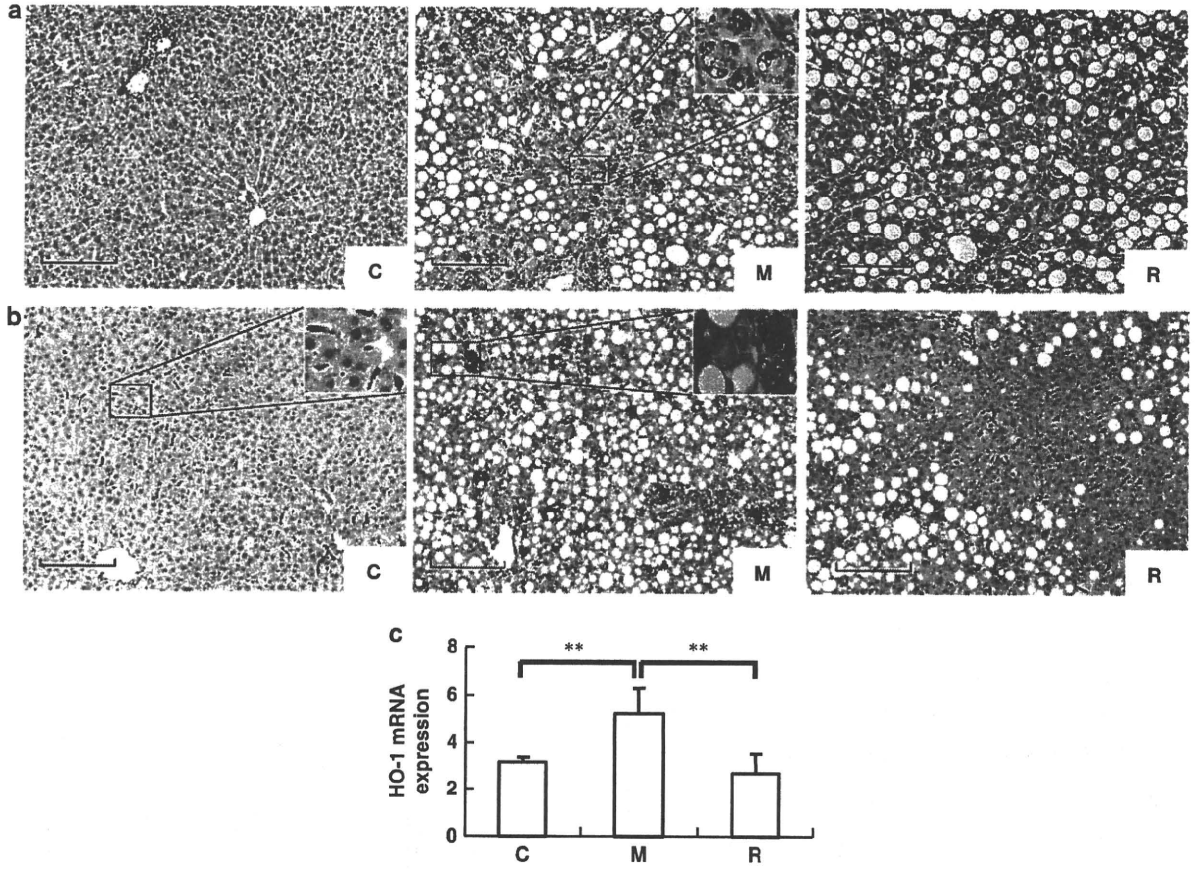

Figure 3 Immunohistochemistry of 4-HNE and HO-1, and the expression of HO-1 mRNA. (**a**) Immunohistochemistry of 4-HNE (× 200). Bar, 25 μm. There is a magnified view of the squared area (× 1000). Foamed macrophages are evident. (**b**) Immunohistochemistry of HO-1 (× 200). The box shows a higher magnification of the squared area. Bar, 25 μm. (**c**) HO-1 mRNA level. $^{**}P<0.01$. The HO-1 mRNA level was normalized by the GAPDH mRNA level.

Conversely, the *in situ* BrdU incorporation assay showed that the number of proliferated hepatocytes underwent no marked changes in group M compared with group C (7.5 ± 3 *vs* 7.6 ± 1.0 cells per field, respectively, $P>0.05$), whereas it increased significantly in group R (17.2 ± 4.35 cells per field) (Figure 5b and d). Furthermore, the ratio of hepatocyte proliferation (BrdU-positive cells)/apoptosis (TUNEL-positive cells) decreased significantly in group M compared with control group C (0.10 ± 0.03 *vs* 0.19 ± 0.03, respectively, $P<0.01$), whereas it increased significantly in group R compared with group M (0.41 ± 0.09, $P<0.01$, Figure 5e). In addition, as shown in Figure 5f, mRNA expression of IL-6, which is known to initiate hepatocyte growth through the STAT3 transcription factor, markedly decreased in group M and thereafter increased in group R, whereas STAT-3 expression remained unchanged (data not shown). Furthermore, mRNA expression of BAX and BAK, proapoptotic genes, markedly increased in group M and returned to the normal range in group R, whereas Bcl-xl and Bcl-2 mRNA expression remained unchanged (data not shown). These results suggest that hepatocyte proliferation/apoptosis undergoes a dynamic transition on changing the diet from MCDD to CD.

Involvement of ER Stress in Fibrosis of Steatohepatitis and its Recovery

Caspase-12 is known as a member of the IL-1β-converting enzyme subfamily of caspases. In rodents, the homolog of this gene mediates apoptosis in response to ER stress. Immunohistochemistry using anti-caspase-12 antibodies revealed that caspase-12 showed negligible expression in group C, whereas it was abundant in hepatocytes with fatty degeneration in group M, indicating the occurrence of ER stress in fatty hepatocytes (Figure 6a). The dietary change clearly reduced the content of caspase-12 in hepatocytes (Figure 6a).

Immunoblot analyses of ER stress-marker proteins such as caspase-12, caspase-7 and cleaved caspase-7, and GRP78 showed that all of these protein expressions were significantly increased in group M and successively reduced in group R (Figure 6b and c). In addition, PDI, an ER-residing protein that catalyzes protein folding and thiol-disulfide interchange reactions,[30,31] was markedly induced in group M compared with groups C and R (Figure 6d).

RT-PCR analyses supported these observations by showing that mRNAs of GRP78, caspase-12, caspase-7, c-Jun, and

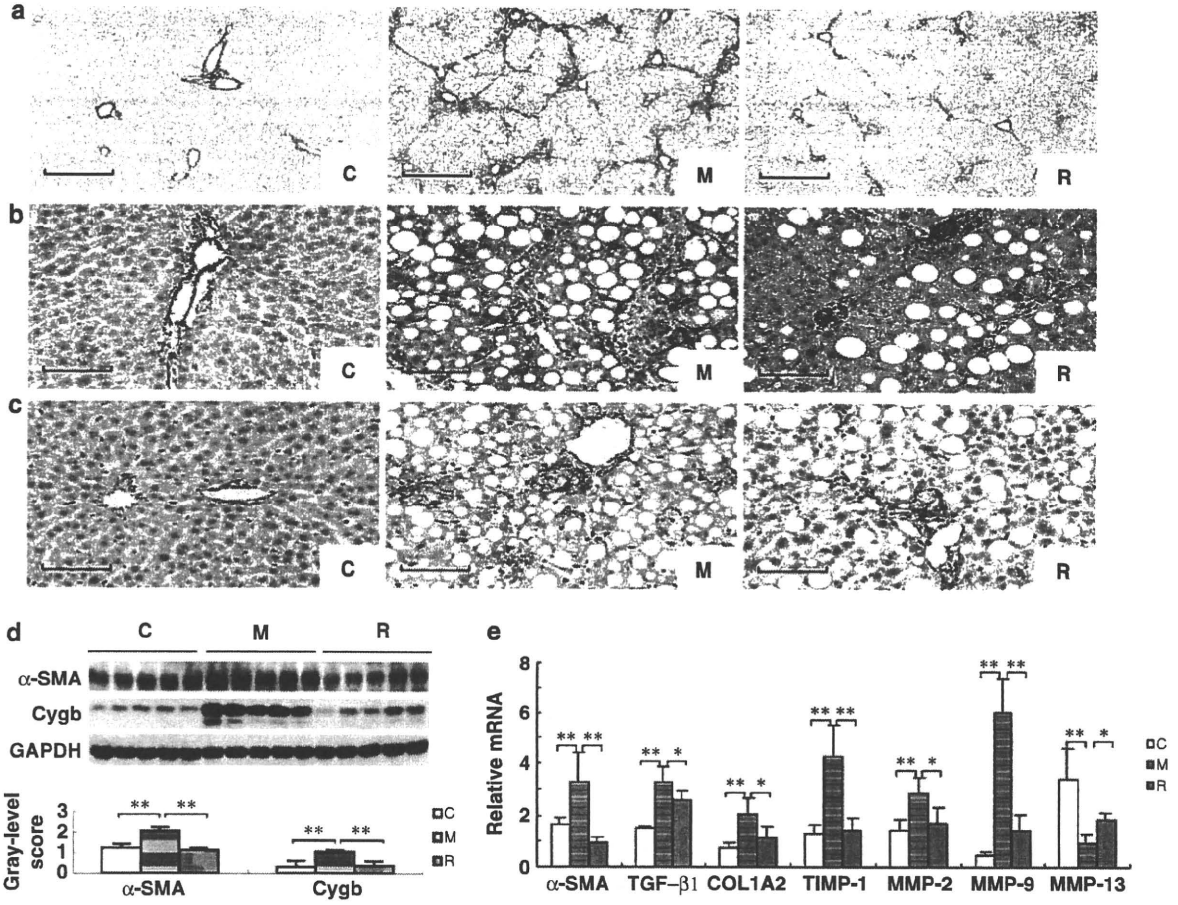

Figure 4 Hepatic stellate cell activation and liver fibrosis. (**a**) Sirius Red staining (× 100). Bar, 50 μm. (**b**) α-SMA immunostaining (× 400). α-SMA-positivity was seen only around large vessels in group C. In group M, α-SMA-positive cells colocalized in and around granulomas close to fatty hepatocytes and perisinusoidal spaces, indicating they were activated stellate cells. The number of α-SMA-positive cells was clearly reduced in group R. Bar, 12.5 μm. (**c**) Cygb immunostaining (× 400). Cygb-positivity was seen only along sinusoids in group C. In group M, Cygb-positive cells colocalized in and around granulomas close to fatty hepatocytes and perisinusoidal spaces, indicating that they were activated stellate cells. The number of Cygb-positive cells was clearly reduced in group R. Bar, 12.5 μm. (**d**) Immunoblotting for α-SMA and Cygb. The gray-level score indicates the histogram of immunoblotting for α-SMA and Cygb. $^{**}P<0.01$. (**e**) Fibrotic gene expressions in the liver determined by qRT-PCR. Relative mRNA levels of α-SMA, TGFβ1, Col1A2, TIMP-1, MMP-2, MMP-9, and MMP-13. mRNA levels were normalized by GAPDH. $^{*}P<0.05$, $^{**}P<0.01$.

ERp57 increased significantly in group C and decreased after 2 weeks of CD diet administration (Figure 6e).

DISCUSSION

Hepatic Steatosis: the 'Primer' for Fibrosis of NASH Induced by MCDD

As both methionine and choline are essential precursors of hepatic phosphatidylcholine synthesis, their deficiency provokes hepatic steatosis by limiting the availability of its substrates, which, in turn, inhibits VLDL assembly and blocks TG secretion from hepatocytes.[32,33] Our study showed that serum levels of TG and FFA in MCDD-induced fatty liver fibrosis (group M) decreased to one-fifth and two-thirds, respectively, of that in the CD group (group C), indicating the impaired secretion of TG and FFA from hepatocytes. Hepatic steatosis facilitates the mitochondrial uptake of FFA, the overflow of which triggers β-oxidation, resulting in the generation of reactive oxygen radicals to trigger lipid peroxidation.[34,35] This leads to the production of toxic substances that damage the mitochondria and stimulate further production of reactive oxygen species.[34] Such a positive feedback loop results in cellular damage, activation of liver macrophages (Kupffer cells), and generation of proinflammatory cytokines that initiate hepatic inflammation.[36,37]

Kupffer cells could be the main source of TNF-α in MCDD-induced liver injury. In addition, MMP-9 (gelatinase B), a member of MMPs, is derived mainly from Kupffer cells in the liver,[38] and its expression is significantly increased together with the activation of cells, indicating that MMP-9 could be a marker of Kupffer cell activation instead of its activity as a collagenase. A number of studies have shown increased serum and plasma levels of MMP-9 in various types

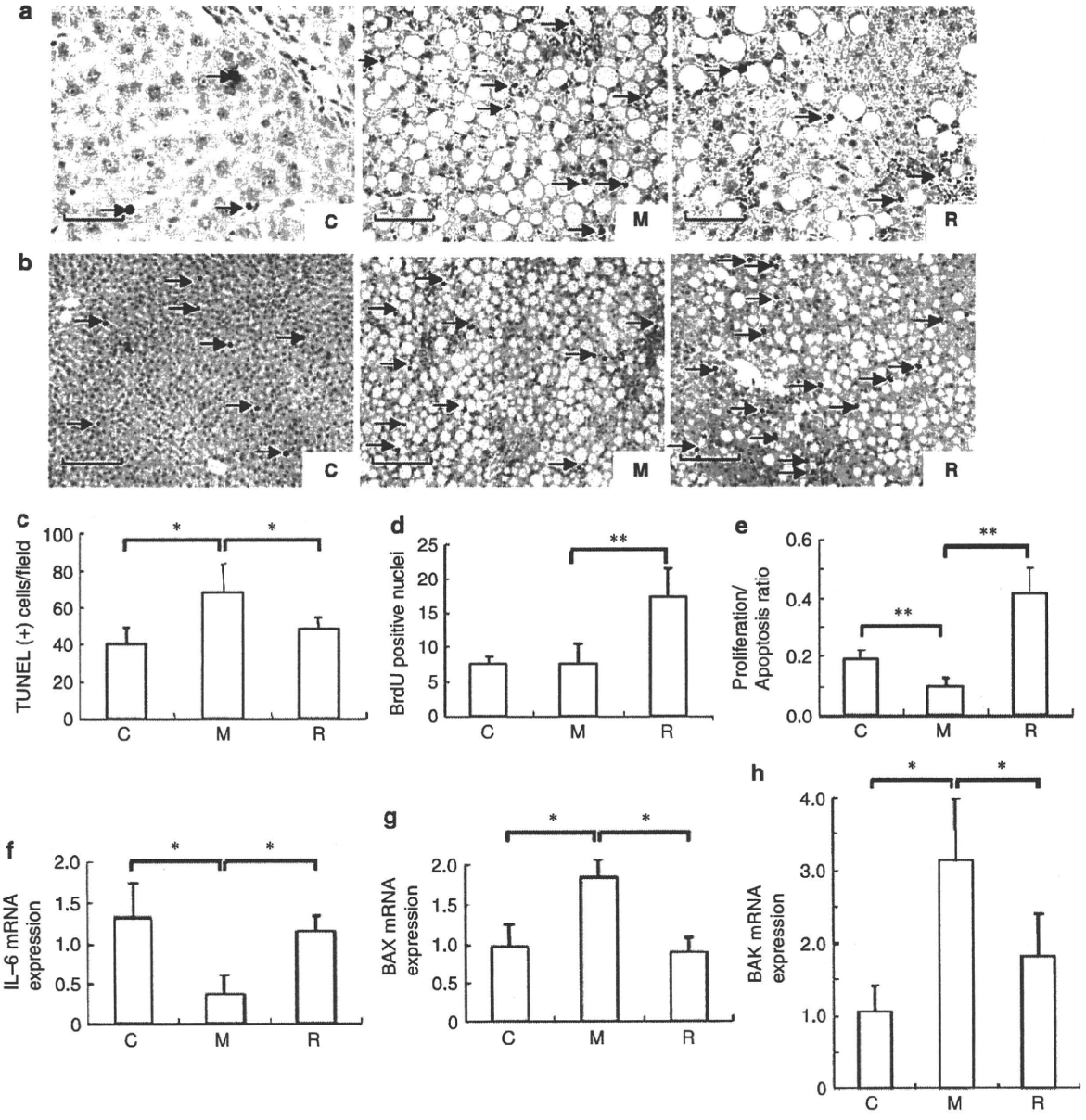

Figure 5 Changes in hepatocyte apoptosis and proliferation. (**a**) A typical photograph of apoptotic hepatocytes (TUNEL staining, arrows) (× 400). TUNEL-positive cells were counted under a microscope in > 100 unselected 20 × microscopic fields per liver. Bar, 12.5 μm. (**b**) A typical photograph of proliferating hepatocytes (BrdU staining, arrows) (× 200). Bar, 25 μm. (**c**) Bar graphs indicate the number of TUNEL-positive cells per field. $^{*}P<0.05$. (**d**) Bar graphs indicate the number of BrdU-positive cells per field. $^{**}P<0.01$. (**e**) The ratio of proliferation/apoptosis of hepatocytes. $^{*}P<0.05$. $^{**}P<0.01$. (**f–h**) Levels of IL-6, BAX, and BAK mRNA. The IL-6, BAX, and BAK mRNA levels determined by RT-PCR. The mRNA level was normalized by the GAPDH mRNA level. $^{**}P<0.01$.

of liver injury, including ischemic reperfusion injury[39] and chronic viral hepatitis.[40,41] Furthermore, the mutation of MMP-9 was reported to inhibit hepatic fibrogenesis in mice.[42] This study showed that MMP-9 and TNF-α mRNA expression increased significantly with the activation of Kupffer cells that were positive for CD68 in group M, whereas switching the diet from MCDD to CD triggered the immediate recovery of MMP-9, suggesting that MMP-9 is associated with the activation status of Kupffer cells.

In contrast, Kupffer cells have been reported to have an important role in the regression of fibrosis through the expression of MMP-13 in other experimental models.[43,44] The current study showed that the number of CD68- and HO-1-positive cells, which are identical to activated Kupffer cells, significantly increased in group M, whereas MMP-13 mRNA expression markedly decreased. Switching the diet from MCDD to CD triggered the immediate recovery of the liver histology, accompanied by a marked increase in the expression

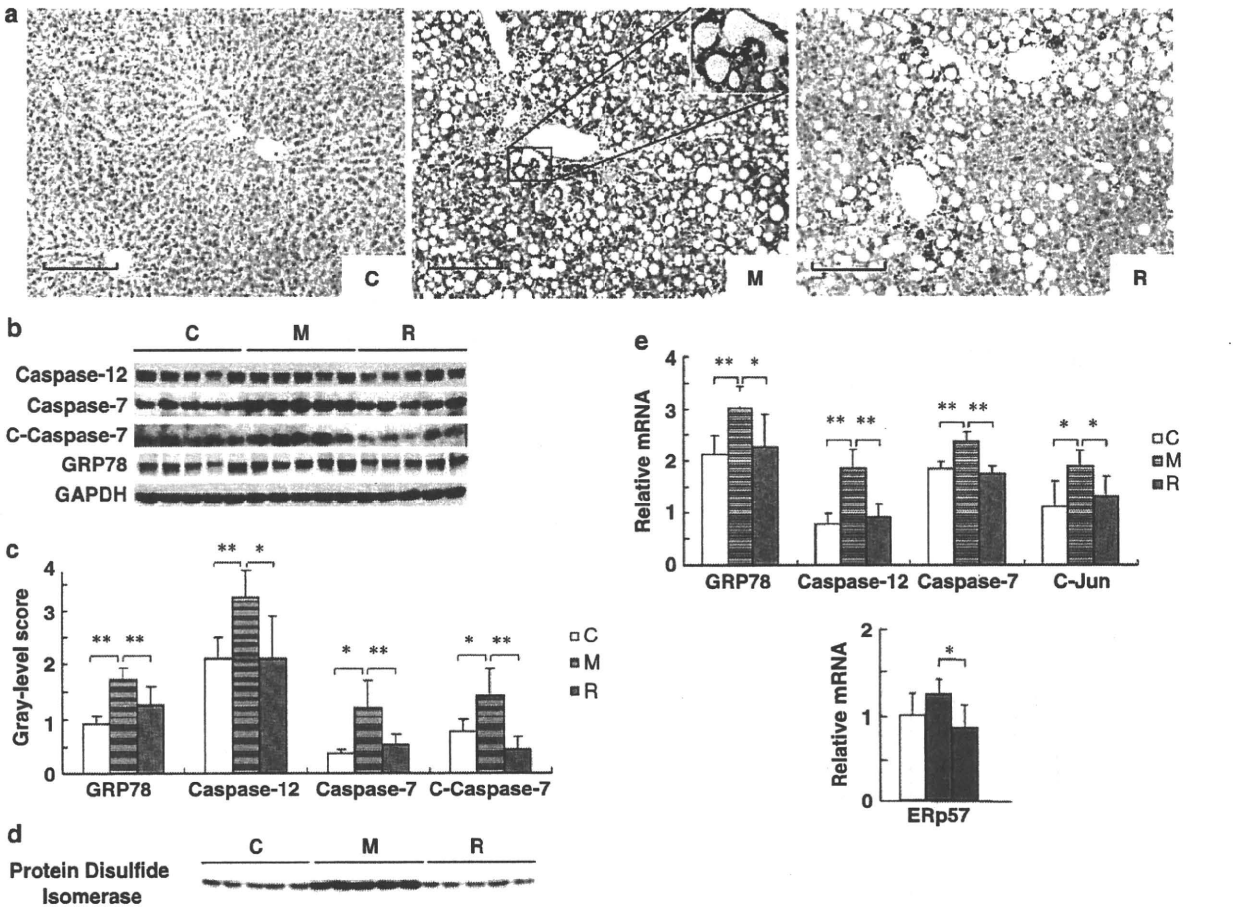

Figure 6 Endoplasmic reticulum stress. (**a**) Caspase-12 immunostaining. Caspase-12-positive cells were rare in group C, whereas hepatocytes with fatty degeneration exhibited caspase-12 positivity in group M. In group R, caspase-12 was retained in hepatocytes with fat, whereas it disappeared in intact hepatocytes. Bar, 25 μm. The box shows an enlarged view of caspase-12-positive hepatocytes with fatty degeneration. (**b**) Immunoblotting of caspase-12, caspase-7, cleaved caspase-7, and GRP78. (**c**) The gray-level score determined by densitometry of the bands on immunoblotting for GRP78, caspase-12, caspase-7, and cleaved caspase-7. (**d**) Immunoblotting of protein disulfide isomerase. (**e**) Relative mRNA levels of GRP78, caspase-12, caspase-7, c-Jun, and ERp57 in groups C, M, and R. mRNA levels were normalized by GAPDH. $^{*}P<0.05$, $^{**}P<0.01$.

of MMP-13 mRNA, indicating the active role of MMP-13 derived from Kupffer cells in the regression of liver fibrosis.[45]

Stellate Cell Activation: a Crucial Role in Fibrosis Development in NASH

Hepatic stellate cells are present in the normal liver in a quiescent state, and their major function seems to be the storage of vitamin A. After injury, stellate cells activate or trans-differentiate into proliferating myofibroblast-like cells that produce abundant levels of fibrillar collagen and TIMP-1.[46] The secretion of abundant levels of TIMP-1 by activated stellate cells inhibits hepatic collagenase activity, and thereby promotes a net increase in extracellular matrix materials. TIMP-1 also promotes hepatic fibrogenesis by inhibiting the apoptosis of activated stellate cells.[47] MMP-2 (gelatinase A), derived mainly from activated stellate cells, is involved in degradation of the basement membrane in the early stage of liver fibrosis.[48] This study showed that both hepatic collagen deposition and stellate cell activation markers, such as α-SMA and cytoglobin, increased significantly with a markedly elevated expression of Col1A2, TIMP-1, MMP-2, and TGFβ-1 mRNAs. After switching to CD feeding, hepatic collagen deposition decreased significantly, accompanied by the marked reduction of these mRNAs, suggesting that MCDD-induced fatty liver fibrosis was closely related to stellate cell activation.

ER Stress: an Important Participant in Advancement of Liver Fibrosis in NASH

Obesity is associated with the induction of ER stress predominantly in the liver and adipose tissues.[49] Previous research has shown that fatty liver induced by a high sucrose

diet and high saturated fat diet shows clear ER stress events in a rodent model.[50] In addition, CHOP (a key component in ER stress-mediated apoptosis) deficiency attenuates cholestasis-induced liver fibrosis by reducing hepatocyte injury in bile duct ligation mice.[51] However, the roles of ER stress in fatty liver induced by MCDD have not been reported. Initial mediators of ER stress responses are ER resident type I transmembrane serine/threonine protein kinases, PKR-like ER kinase, and inositol-requiring enzyme-1(IRE-1); the accumulation of unfolded proteins in ER induces the oligomerization-dependent autophosphorylation of these kinases,[52,53] and thereby initiates cytoplasmic signal transduction. It was recently shown that activated IRE-1 on the ER membrane recruits TNF receptor-associated factor 2, and thus activates c-Jun amino-terminal kinase.[54] In addition, the survival response activates genes that encode ER-residing chaperones such as GRP78/Bip, which uses energy derived from ATP hydrolysis to prevent the aggregation of ER proteins and is considered the classical marker of UPR activation.[55] The current study showed that the expression of ER stress markers GRP78 (protein and mRNA) and c-Jun mRNA increased significantly in the MCDD group, whereas the expression of all of them decreased markedly after changing the diet. Another ER stress-related molecule, PDI,[30,31] showed similar behavior (Figure 6d and e). Thus, ER stress may be a key factor in MCDD-induced fatty liver fibrosis.

Caspases also participate in ER stress-induced apoptosis. In mice, procaspase-12 is localized on the cytoplasmic side of the ER and is cleaved and activated specifically by ER stress, but not by death receptor or mitochondria-mediated apoptotic signals.[56] Caspase-7, which translocates from the cytosol to the cytoplasmic side of the ER membrane in response to ER stress, has been reported to interact with and cleave procaspase-12, leading to its activation.[57] Activated caspase-12 then cleaves and activates procaspase-9, which in turn activates the downstream caspase cascade, including caspase-3, DNA fragmentation, and cell death.[58] Our results also showed that protein and gene expressions of caspase-12, caspase-7, and cleaved caspase-7 were significantly elevated during steatohepatitis together with the increased number of apoptotic hepatocytes, whereas they were reduced markedly after changing the diet. Furthermore, although the proliferation of hepatocytes did not show a clear change in the MCDD group, the ratio of hepatocyte proliferation/apoptosis decreased significantly, whereas it increased markedly after changing the diet to CD, indicating that the apoptotic caspase-12 pathway may also inhibit hepatocyte proliferation in MCDD-induced steatohepatitis. The marked elevation of BAX and BAK may also participate in stimulating the apoptosis of hepatocytes by MCDD.

In conclusion, this study shows that, although the underlying mechanisms involved in MCDD-induced fatty liver fibrosis are complicated, they may include not only well-known factors, such as steatosis, oxidative stress, and the activation of Kupffer and stellate cells, but also ER stresses and the balance between hepatocyte proliferation and apoptosis. The reversibility of liver fibrosis is also shown in steatohepatitis, at least in the present MCDD model.

Supplementary Information accompanies the paper on the Laboratory Investigation website (http://www.laboratoryinvestigation.org)

ACKNOWLEDGEMENTS

NK was supported by a Grant-in-Aid for Scientific Research from the Japan Society for the Promotion of Science through Grant no. 18659214 (2007), by a Grant for Research on Hepatitis from the Ministry of Health, Labour and Welfare (2008), and by a Trust Area Research Grant from Osaka City University (2008). We thank Dr Ryoko Shiga for her valuable discussion about this paper.

DISCLOSURE/CONFLICT OF INTEREST

The authors declare no conflict of interest.

1. Angulo P. Nonalcoholic fatty liver disease. N Engl J Med 2002; 346:1221–1231.
2. Clark JM, Diehl AM. Hepatic steatosis and type 2 diabetes mellitus. Curr Diab Rep 2002;2:210–215.
3. Festi D, Colecchia A, Sacco T, *et al.* Hepatic steatosis in obese patients: clinical aspects and prognostic significance. Obes Rev 2004;5:27–42.
4. Bedogni G, Miglioli L, Masutti F, *et al.* Prevalence of and risk factors for nonalcoholic fatty liver disease: the Dionysos nutrition and liver study. Hepatology 2005;42:44–52.
5. Boccato S, Pistis R, Noventa F, *et al.* Fibrosis progression in initially mild chronic hepatitis C. J Viral Hepat 2006;13:297–302.
6. Fartoux L, Chazouillères O, Wendum D, *et al.* Impact of steatosis on progression of fibrosis in patients with mild hepatitis C. Hepatology 2005;41:82–87.
7. Leandro G, Mangia A, Hui J, *et al.* Relationship between steatosis, inflammation and fibrosis in chronic hepatitis C: a meta-analysis of individual patient data. Gastroenterology 2006;130:1636–1642.
8. Sass DA, Chang P, Chopra KB. Nonalcoholic fatty liver disease: a clinical review. Dig Dis Sci 2005;50:171–180.
9. Bugianesi E, Leone N, Vanni E, *et al.* Expanding the natural history of nonalcoholic steatohepatitis: from cryptogenic cirrhosis to hepatocellular carcinoma. Gastroenterology 2002;123:134–140.
10. Shimada M, Hashimoto E, Taniai M, *et al.* Hepatocellular carcinoma in patients with non-alcoholic steatohepatitis. J Hepatol 2002;37: 154–160.
11. Bugianesi E. Review article: steatosis, the metabolic syndrome and cancer. Aliment Pharmacol Ther 2005;22(Suppl 2):40–43.
12. Kelley DE, McKolanis TM, Hegazi RA, *et al.* Fatty liver in type 2 diabetes mellitus: relation to regional adiposity, fatty acids, and insulin resistance. Am J Physiol Endocrinol Metab 2003;285:E906–E916.
13. Shiratori Y, Imazeki F, Moriyama M, *et al.* Histologic improvement of fibrosis in patients with hepatitis C who have sustained response to interferon therapy. Ann Intern Med 2000;132:517–524.
14. Poynard T, McHutchison J, Davis GL, *et al.* Impact of interferon alfa-2b and ribavirin on progression of liver fibrosis in patients with chronic hepatitis C. Hepatology 2000;32:1131–1137.
15. Yuan M, Konstantopoulos N, Lee J, *et al.* Reversal of obesity- and diet-induced insulin resistance with salicylates or targeted disruption of Ikkbeta. Science 2001;293:1673–1677.
16. Uysal KT, Wiesbrock SM, Marino MW, *et al.* Protection from obesity-induced insulin resistance in mice lacking TNF-alpha function. Nature 1997;389:610–614.
17. Hirosumi J, Tuncman G, Chang L, *et al.* A central role for JNK in obesity and insulin resistance. Nature 2002;420:333–336.
18. Hampton RY. ER stress response: getting the UPR hand on misfolded proteins. Curr Biol 2000;10:R518–R521.
19. Mori K. Tripartite management of unfolded proteins in the endoplasmic reticulum. Cell 2000;101:451–454.
20. Harding HP, Calfon M, Urano F, *et al.* Transcriptional and translational control in the mammalian unfolded protein response. Annu Rev Cell Dev Biol 2002;18:575–599.

21. Ji C, Kaplowitz N. Betaine decreases hyperhomocysteinemia, endoplasmic reticulum stress, and liver injury in alcohol-fed mice. Gastroenterology 2003;124:1488–1499.
22. Rodrigues CM, Ma X, Linehan-Stieers C, *et al.* Ursodeoxycholic acid prevents cytochrome c release in apoptosis by inhibiting mitochondrial membrane depolarization and channel formation. Cell Death Differ 1999;6:842–854.
23. Pavio N, Romano PR, Graczyk TM, *et al.* Protein synthesis and endoplasmic reticulum stress can be modulated by the hepatitis C virus envelope protein E2 through the eukaryotic initiation factor 2 alpha kinase PERK. J Virol 2003;77:3578–3585.
24. Tardif KD, Mori K, Siddiqui A. Hepatitis C virus subgenomic replicons induce endoplasmic reticulum stress activating an intracellular signaling pathway. J Virol 2002;76:7453–7459.
25. Kawada N, Kristensen DB, Asahina K, *et al.* Characterization of a stellate cell activation-associated protein (STAP) with peroxidase activity found in rat hepatic stellate cells. J Biol Chem 2001;276:25318–25323.
26. Nakatani K, Seki S, Kawada N, *et al.* Expression of SPARC by activated hepatic stellate cells and its correlation with the stages of fibrogenesis in human chronic hepatitis. Virchows Arch 2002;441:466–474.
27. Otogawa K, Kinoshita K, Fujii H, *et al.* Erythrophagocytosis by liver macrophages (Kupffer cells) promotes oxidative stress, inflammation, and fibrosis in a rabbit model of steatohepatitis: implications for the pathogenesis of human nonalcoholic steatohepatitis. Am J Pathol 2007;170:967–980.
28. Wang YQ, Ikeda K, Ikebe T, *et al.* Inhibition of hepatic stellate cell proliferation and activation by the semisynthetic analogue of fumagillin TNP-470 in rats. Hepatology 2000;32:980–989.
29. Uyama N, Shimahara Y, Okuyama H, *et al.* Carbenoxolone inhibits DNA synthesis and collagen gene expression in rat hepatic stellate cells in culture. J Hepatol 2003;39:749–755.
30. Riemer J, Bulleid N, Herrmann JM. Disulfide formation in the ER and mitochondria: two solutions to a common process. Science 2009;324:1284–1287.
31. Nakamura T, Lipton SA. Cell death: protein misfolding and neurodegenerative diseases. Apoptosis 2009;14:455–468.
32. Vance JE, Vance DE. The role of phosphatidylcholine biosynthesis in the secretion of lipoproteins from hepatocytes. Can J Biochem Cell Biol 1985;63:870–881.
33. Yao ZM, Vance DE. The active synthesis of phosphatidylcholine is required for very low density lipoprotein secretion from rat hepatocytes. J Biol Chem 1988;263:2998–3004.
34. Fromenty B, Robin MA, Igoudjil A, *et al.* The ins and outs of mitochondrial dysfunction in NASH. Diabetes Metab 2004;30:121–138.
35. Pessayre D, Fromenty B. NASH: a mitochondrial disease. J Hepatol 2005;42:928–940.
36. Albano E, Mottaran E, Occhino G, *et al.* Review article: role of oxidative stress in the progression of non-alcoholic steatosis. Aliment Pharmacol Ther 2005;22:71–73.
37. Day CP. From fat to inflammation. Gastroenterology 2006;130:207–210.
38. Winwood PJ, Schuppan D, Iredale JP, *et al.* Kupffer cell-derived 95 kDa type IV collagenase/gelatinase B: characterisation and expression in cultured cells. Hepatology 1995;22:304–315.
39. Kuyvenhoven JP, Verspaget HW, Gao Q, *et al.* Assessment of serum matrix metalloproteinases MMP-2 and MMP-9 after human liver transplantation: increased serum MMP-9 level in acute rejection. Transplantation 2004;77:1646–1652.
40. Leroy V, Monier F, Bottari S, *et al.* Circulating matrix metalloproteinases 1, 2, 9 and their inhibitors TIMP-1 and TIMP-2 as serum markers of liver fibrosis in patients with chronic hepatitis C: comparison with PIIINP and hyaluronic acid. Am J Gastroenterol 2004;799:271–279.
41. Chung TW, Kim JR, Suh JI, *et al.* Correlation between plasma levels of matrix metalloproteinase (MMP)-9/MMP-2 ratio and alpha-fetoproteins in chronic hepatitis carrying hepatitis B virus. J Gastroenterol Hepatol 2004;19:565–571.
42. Roderfeld M, Weiskirchen R, Wagner S, *et al.* Inhibition of hepatic fibrogenesis by matrix metalloproteinase-9 mutants in mice. FASEB J 2006;20:444–454.
43. Hironaka K, Sakaida I, Matsumura Y, *et al.* Enhanced interstitial collagenase (matrix metalloproteinase-13) production of Kupffer cell by gadolinium chloride prevents pig serum-induced rat liver fibrosis. Biochem Biophys Res Commun 2000;267:290–295.
44. Sakaida I, Hironaka K, Terai S, *et al.* Gadolinium chloride reverses dimethylnitrosamine (DMN)-induced rat liver fibrosis with increased matrix metalloproteinases (MMPs) of Kupffer cells. Life Sci 2003;72:943–959.
45. Friedman S. Mac the knife? Macrophages —the double-edged sword of hepatic fibrosis. J Clin Invest 2005;115:29–32.
46. Iredale JP, Benyon RC, Arthur MJ, *et al.* Tissue inhibitor of metalloproteinase-1 messenger RNA expression is enhanced relative to interstitial collagenase messenger RNA in experimental liver injury and fibrosis. Hepatology 1996;24:176–184.
47. Iredale JP, Murphy G, Hembry RM, *et al.* Human hepatic lipocytes synthesize tissue inhibitor of metalloproteinases-1. Implications for regulation of matrix degradation in liver. J Clin Invest 1992;90:282–287.
48. Winwood PJ, Schuppan D, Iredale JP, *et al.* Kupffer cell-derived 95-kd type IV collagenase/gelatinase B: characterization and expression in cultured cells. Hepatology 1995;22:304–315.
49. Ozcan U, Cao Q, Yilmaz E, *et al.* Hotamisligil. Endoplasmic reticulum stress links obesity, insulin action, and type 2 diabetes. Science 2004;306:457–461.
50. Wang D, Wei Y, Pagliassotti MJ. Saturated fatty acids promote endoplasmic reticulum stress and liver injury in rats with hepatic steatosis. Endocrinology 2006;147:943–951.
51. Tamaki N, Hatano E, Taura K, *et al.* CHOP deficiency attenuates cholestasis-induced liver fibrosis by reduction of hepatocyte injury. Am J Physiol Gastrointest Liver Physiol 2008;294:G498–G505.
52. Bertolotti A, Zhang Y, Hendershot LM, *et al.* Dynamic interaction of BiP and ER stress transducers in the unfolded-protein response. Nat Cell Biol 2000;2:326–332.
53. Liu CY, Schröder M, Kaufman RJ. Ligand-independent dimerization activates the stress response kinases IRE1 and PERK in the lumen of the endoplasmic reticulum. J Biol Chem 2000;275:24881–24885.
54. Urano F, Wang X, Bertolotti A, *et al.* Coupling of stress in the ER to activation of JNK protein kinases by transmembrane protein kinase IRE1. Science 2000;287:664–666.
55. Iwawaki T, Hosoda A, Okuda T, *et al.* Translational control by the ER transmembrane kinase/ribonuclease IRE1 under ER stress. Nat Cell Biol 2001;3:158–164.
56. Nakagawa T, Yuan J. Cross-talk between two cysteine protease families. Activation of caspase-12 by calpain in apoptosis. J Cell Biol 2000;150:887–894.
57. Rao RV, Hermel E, Castro-Obregon S, *et al.* Coupling endoplasmic reticulum stress to the cell death program: mechanism of caspase activation. J Biol Chem 2001;276:33869–33874.
58. Tan Y, Dourdin N, Wu C, *et al.* Ubiquitous calpains promote caspase-12 and JNK activation during endoplasmic reticulum stress-induced apoptosis. J Biol Chem 2006;281:16016–16024.

Journal of Medical Virology 83:871–878 (2011)

Association of IL28B Variants With Response to Pegylated-Interferon Alpha Plus Ribavirin Combination Therapy Reveals Intersubgenotypic Differences Between Genotypes 2a and 2b

Naoya Sakamoto, MD, PhD,[1,2]* Mina Nakagawa,[1] Yasuhito Tanaka,[3] Yuko Sekine-Osajima,[1] Mayumi Ueyama,[1] Masayuki Kurosaki,[4] Nao Nishida,[5] Akihiro Tamori,[6] Nishimura-Sakurai Yuki,[1] Yasuhiro Itsui,[1,7] Seishin Azuma,[1] Sei Kakinuma,[1,2] Shuhei Hige,[8] Yoshito Itoh,[9] Eiji Tanaka,[10] Yoichi Hiasa,[11] Namiki Izumi,[4] Katsushi Tokunaga,[5] Masashi Mizokami,[12] Mamoru Watanabe[1] and the Ochanomizu-Liver Conference Study Group

[1]*Department of Gastroenterology and Hepatology, Tokyo Medical and Dental University, Tokyo, Japan*
[2]*Department for Hepatitis Control, Tokyo Medical and Dental University, Tokyo, Japan*
[3]*Department of Virology & Liver Unit, Nagoya City University Graduate School of Medical Sciences, Mizuho-ku Nagoya, Japan*
[4]*Division of Gastroenterology and Hepatology, Musashino Red Cross Hospital, Tokyo, Japan*
[5]*Department of Human Genetics, Graduate School of Medicine, The University of Tokyo, Tokyo, Japan*
[6]*Department of Hepatology, Osaka City University Graduate School of Medicine, Osaka, Japan*
[7]*Department of Internal Medicine, Soka Municipal Hospital, Saitama, Japan*
[8]*Department of Internal Medicine, Hokkaido University Graduate School of Medicine, Sapporo, Japan*
[9]*Molecular Gastroenterology and Hepatology, Kyoto Prefectural University of Medicine, Kyoto, Japan*
[10]*Department of Medicine, Shinshu University School of Medicine, Matsumoto, Japan*
[11]*Department of Gastroenterology and Metabology, Ehime University Graduate School of Medicine, Ehime, Japan*
[12]*Research Center for Hepatitis and Immunology, International Medical Center of Japan Konodai Hospital, Ichikawa, Japan*

Genetic polymorphisms of the interleukin 28B (IL28B) locus are associated closely with outcomes of pegylated-interferon (PEG-IFN) plus ribavirin (RBV) combination therapy. The aim of this study was to investigate the relationship between IL28B polymorphism and responses to therapy in patients infected with genotype 2. One hundred twenty-nine chronic hepatitis C patients infected with genotype 2, 77 patients with genotype 2a and 52 patients with genotype 2b, were analyzed. Clinical and laboratory parameters, including genetic variation near the IL28B gene (rs8099917), were assessed. Drug adherence was monitored in each patient. Univariate and multivariate statistical analyses of these parameters and clinical responses were carried out. Univariate analyses showed that a sustained virological response was correlated significantly with IL28B polymorphism, as well as age, white blood cell and neutrophil counts, adherence to RBV, and rapid virological response. Subgroup analysis revealed that patients infected with genotype 2b achieved significantly lower rapid virological response rates than those with genotype 2a. Patients with the IL28B-major allele showed higher virus clearance rates at each time point than those with the IL28B-minor allele, and the differences were more profound in patients infected with genotype 2b than those with genotype 2a. Furthermore, both rapid and sustained virological responses were associated significantly with IL28B alleles in patients with genotype

Abbreviations: HCV, hepatitis C virus; HCC, hepatocellular carcinoma; IFN, interferon; PEG-IFN, pegylated-interferon; RBV, ribavirin; IL28B, interleukin 28B; SNPs, single nucleotide polymorphisms; BMI, body mass index; ALT, alanine transaminase; ISDR, the interferon sensitivity determining region; ITPA, inosine triphosphatase

Grant sponsor: Ministry of Education, Culture, Sports, Science and Technology-Japan; Grant sponsor: Japan Society for the Promotion of Science, Ministry of Health, Labour and Welfare-Japan; Grant sponsor: Japan Health Sciences Foundation; Grant sponsor: Miyakawa Memorial Research Foundation; Grant sponsor: National Institute of Biomedical Innovation.

Naoya Sakamoto and Mina Nakagawa contributed equally to this work.

*Correspondence to: Naoya Sakamoto, MD, PhD, Department of Gastroenterology and Hepatology, Tokyo Medical and Dental University, 1-5-45 Yushima, Bunkyo-ku, Tokyo 113-8519, Japan. E-mail: nsakamoto.gast@tmd.ac.jp

Accepted 10 January 2011

DOI 10.1002/jmv.22038
Published online in Wiley Online Library (wileyonlinelibrary.com).

2b. IL28B polymorphism was predictive of PEG-IFN plus RBV combination treatment outcomes in patients infected with genotype 2 and, especially, with genotype 2b. In conclusion, IL-28B polymorphism affects responses to PEG-IFN-based treatment in difficult-to-treat HCV patients. ***J. Med. Virol. 83:871–878, 2011.*** © 2011 Wiley-Liss, Inc.

KEY WORDS: hepatitis C virus (HCV); chronic hepatitis C; genotype 2; PEG-IFN plus RBV therapy; combination therapy; IL28B; interferon-λ3

INTRODUCTION

Hepatitis C virus (HCV) infects around 170 million people worldwide and is characterized by a high probability of developing chronic inflammation and fibrosis of the liver, leading to end-stage liver failure and hepatocellular carcinoma (HCC) [Alter, 1997; Sakamoto and Watanabe, 2009]. Since the first report in 1986, type I interferons have been the mainstay of HCV therapy [Hoofnagle, 1994]. Current standards of care consist of a combination of ribavirin (RBV) plus pegylated interferon (PEG-IFN)-alpha for 48 weeks for infection with genotypes 1 and 4, and for 24 weeks for the other genotypes [Zeuzem et al., 2000; Fried et al., 2002]. Although this treatment improved substantially sustained virological response rates, it may result also in serious adverse effects and a considerable proportion of patients require early discontinuation of treatment. Patients of African origin have even poorer treatment outcomes [Rosen and Gretch, 1999]. Given this situation, a precise assessment of the likely treatment outcomes before the initiation of treatment may improve substantially the quality of antiviral treatment.

Recently, several studies have reported that genetic polymorphisms of the IL28B locus, which encodes interferon-λ3 (interleukin 28B), are associated with response to interferon-based treatment of chronic HCV infections with genotype 1 [Ge et al., 2009; Suppiah et al., 2009; Tanaka et al., 2009] and also spontaneous clearance of HCV [Thomas et al., 2009].

While chronic HCV infections with genotype 2 are associated with good treatment outcome, there are some refractory cases among patients infected with genotype 2, similar to genotype 1. The aims of this study were to analyze retrospectively clinical and virological factors associated with treatment response in patients with chronic HCV infection with genotype 2 who were treated with PEG-IFN plus RBV combination therapy and to clarify the relationship between IL28B polymorphism and the response to combination therapy.

PATIENTS AND METHODS

The authors analyzed retrospectively 129 patients with chronic HCV infection with genotype 2 who received combination therapy with PEG-IFN plus RBV between December 2004 and December 2009 at 10 multicenter hospitals (liver units with hepatologists) throughout Japan. All patients had chronic active hepatitis confirmed histologically or clinically and were positive for anti-HCV antibodies and serum HCV RNA by quantitative or qualitative assays. Patients with a positive test for serum hepatitis B surface antigen, coinfection with other HCV genotypes, coinfection with human immunodeficiency virus, other causes of hepatocellular injury (such as alcoholism, autoimmune hepatitis, primary biliary cirrhosis, or a history of treatment with hepatotoxic drugs), and a need for hemodialysis were excluded.

Study Design

Each patient was treated with combination therapy with PEG-IFN-α2b (Peg-Intron, Schering-Plough Nordic Biotech, Stockholm, Sweden, at a dose of 1.2–1.5 μg/kg subcutaneously once a week) or PEG-IFN-α2a (Pegasys; Roche, Basel, Switzerland, at a dose of 180 μg subcutaneously once a week) plus RBV (Rebetol, Schering-Plough Nordic Biotech or Copegus; Roche) 600–1,000 mg daily depending on the body weight (b.w.) (b.w. <60 kg: 600 mg po daily; b.w: 60–80 kg: 800 mg po daily; b.w. >80 kg: 1,000 mg po daily; in two divided doses). The duration of the combination therapy was set at a standard 24 weeks, but treatment reduction or discontinuation was permitted by doctor's decision. The rates of PEG-IFN and RBV administration achieved were calculated as percentages of actual total dose administered of a standard total dose of 24 weeks, according to body weight before therapy. During treatment, patients were assessed as outpatients at weeks 2, 4, 6, 8, and then every 4 weeks for the duration of treatment and at every 4 weeks after the end of treatment. Biochemical and hematological testing was carried out in a central laboratory. Serum HCV RNA was measured before treatment, during treatment at 4 weekly intervals, and after therapy at 4 weekly intervals for 24 weeks, by quantitative or qualitative assays.

Patient Evaluation

The following factors were analyzed to determine whether they were related to the efficacy of combination therapy: age, gender, body mass index (BMI), previous IFN therapy, grade of inflammation and stage of fibrosis on liver biopsy, pretreatment biochemical parameters, such as white blood cells, neutrophils, hemoglobin, platelet count, alanine transaminase (ALT) level, serum HCV RNA level (log IU/ml), and single nucleotide polymorphism (SNPs) in the *IL28B* locus (rs8099917). Liver biopsy specimens were evaluated blindly, to determine the grade of inflammation and stage of fibrosis, by an independent interpreter who was not aware of the clinical data. Activity of inflammation was graded on a scale of 0–3: A0 shows no activity, A1 shows mild activity, A2 shows moderate activity and A3 shows severe activity. Fibrosis was staged on a scale of 0–4:

F0 shows no fibrosis, F1 shows moderate fibrosis, F2 shows moderate fibrosis with few septa, F3 shows severe fibrosis with numerous septa without cirrhosis and F4 shows cirrhosis.

Informed written consent was obtained from each patient who participated in the study. The study protocol conformed to the ethical guidelines of the Declaration of Helsinki and to the relevant ethical guidelines as reflected in a priori approval by the ethics committees of all the participating universities and hospitals.

SNP Genotyping

Human genomic DNA was extracted from whole blood of each patient. Genetic polymorphism of IL28B was determined by DigiTag2 assay by typing one tag SNP located within the IL28B locus, rs8099917 (22). Heterozygotes (T/G) or homozygotes (G/G) of the minor allele (G) were defined as having the IL28B minor allele, whereas homozygotes for the major allele (T/T) were defined as having the IL28B major allele.

Outcomes

The primary end point was a sustained biochemical and virological response. A sustained virological response was defined as serum HCV RNA undetectable at 24 weeks after the end of treatment. Secondary end points were a rapid virological response (HCV RNA undetectable in serum at week 4) and end-of-treatment virological response. In addition, tolerability (adverse events) and drug adherence were recorded and factors potentially associated with virological response explored.

Statistical Analysis

SPSS software package (SPSS 18J, SPSS, Chicago, IL) was used for statistical analysis. Discrete variables were evaluated by Fisher's exact probability test and distributions of continuous variables were analyzed by the Mann–Whitney *U*-test. Independent factors possibly affecting response to combination therapy were examined by stepwise multiple logistic-regression analysis. All *P*-values were calculated by two-tailed tests, and those of less than 0.05 were considered statistically significant.

RESULTS

Clinical Characteristics and Response to Therapy

The clinical characteristics and response rates to therapy of 129 patients are summarized in Tables I and II. Sixty-eight patients achieved a rapid virological response, whereas 44 patients remained HCV-RNA positive at week 4. Treatment reduction or cessation was permitted also to avoid side effects, and one patient stopped treatment at week 12 because he was anticipated to be a non-responder. On an intention-to-treat analysis, serum HCV-RNA levels were negative at the end of treatment in 125 of the 129 patients (97%) treated and, among them, 98 (76%) achieved a sustained virological response. The rapid virological response rate of patients infected with genotype 2b was lower significantly than that of patients infected with genotype 2a ($P = 0.036$) (Table II). The sustained virological response rate decreased with RBV drug discontinuation and dose reduction (84% and 66% with ≧80% and <80% of RBV dose, $P = 0.021$, Table III). Adherences to PEG-IFN did not influence a sustained virological response or end of treatment response significantly, while RBV adherence was associated significantly with a sustained virological response (Table III).

TABLE I. Baseline Characteristics of Participating Patients Infected With HCV Genotype 2

Total number	129
Genotype (2a/2b)	77/52
IL28B SNPs (rs8099917)	
TT/TG/GG	100/28/1
Age (years)[a]	64 (20–73)
Gender (male/female)	64/65
Body mass index (kg/m^2)[a] (N = 80)	23.7 (16.9–33.5)
Previous interferon therapy (no/yes)	102/21 (unknown 6)
Histology at biopsy (N = 96)	
Grade of inflammation	
A0/1/2/3	10/53/29/4
Stage of fibrosis	
F0/1/2/3	7/59/19/11
White blood cells (/μl)[b] (N = 94)	5,115 ± 1,630
Neutrophils (/μl)[b] (N = 94)	2,765 ± 1,131
Hemoglobin (g/dl)[b] (N = 95)	14.2 ± 1.3
Platelet count (×10^{-3}/μl)[b] (N = 98)	187 ± 95
ALT (IU/L)[b] (N = 95)	82 ± 78
Serum HCV-RNA level (log(IU/ml))[a,c]	6.2 (3.6–7.4)
Treatment duration (>16, ≦24)	19/110

SNPs, single nucleotide polymorphisms; ALT, alanine transaminase.
[a]Data are shown as median (range) values.
[b]Data are expressed as mean ± SD.
[c]Data are shown as log(IU/ml)).

Factors Associated With a Sustained Virological Response

Next the host clinical and viral factors associated with a sustained virological response were analyzed. Univariate statistical analysis showed that six parameters were associated significantly with the sustained virological response rates, including age, white blood cells, neutrophils, adherence to RBV, rapid virological response and an IL28B SNP (rs8099917) (Table IV). There was no significant association of sustained virological response with gender, previous interferon therapy, stage of fibrosis, pretreatment HCV titer or adherence to PEG-IFN. Further multivariate analyses were conducted using significant factors identified by the univariate analysis (Table V). The multiple logistic-regression analysis showed that only a rapid virological response was associated with a sustained virological response (OR = 0.170, $P = 0.019$).

TABLE II. Response Rates to Therapy

Character			Number/total number (%)
Overall			
RVR			68/112 (61)
ETR			125/129 (97)
SVR			98/129 (76)
Genotype	2a	2b	*P*-value
RVR	46/67 (69)	22/45 (49)	**0.036**
ETR	74/77 (96)	51/52 (98)	NS
SVR	56/77 (73)	42/52 (81)	NS

RVR, rapid virological response; ETR, end of treatment response; SVR, sustained virological response.
Bold indicated *P*-value of less than 0.05.

TABLE III. Response Rates to Treatment According to Drug Adherence

	≧80%	<80%	*P*-value
PEG-IFN adherence			
ETR	94/96 (98)	31/33 (94)	NS
SVR	75/96 (78)	23/33 (70)	NS
RBV adherence			
ETR	72/73 (99)	53/56 (95)	NS
SVR	61/73 (84)	37/56 (66)	**0.021**

ETR, end of treatment response; SVR, sustained virological response; PEG-IFN, pegylated interferon; RBV, ribavirin.
The rates of PEG-IFN and RBV administration achieved were calculated as percentages of actual total dose administered of a standard total dose of 24 weeks, according to body weight before therapy.
Bold indicated *P*-value of less than 0.05.

Comparison of Sustained Virological Response Rates According to IL28B SNPs

The PEG-IFN plus RBV treatment efficacy was compared after dividing the study subjects into two groups based on IL28B alleles (Table VI). Patients homozygous for the IL28B major allele (TT allele) achieved significantly higher rapid and sustained virological response rates than those heterozygous or homozygous for the IL28B minor allele (TG/GG alleles) ($P < 0.05$). In addition, responses to PEG-IFN plus RBV treatment were analyzed after dividing the study subjects into those with genotype 2a and with genotype 2b. The rapid and sustained virological response rates tended to be higher in patients homozygous for the IL28B major allele than those heterozygous or homozygous for the

TABLE IV. Clinical and Virological Characteristics of Patients Based on Therapeutic Response

	SVR (n = 98)	Non-SVR (n = 31)	*P*-value
Genotype (2a/2b)		56/42	21/10
IL28B SNPs (rs8099917)			
TT/TG + GG	81/17	19/12	**0.024**
Age (years)[a]	56 (20–73)	61 (40–72)	**0.002**
Gender (male/female)	51/47	13/18	NS
Body mass index (kg/m^2)[a]	22.8 (16.9–33.5)	24.1 (20.3–27.6)	NS
Previous Interferon therapy (no/yes)	80/14	22/7	NS
Grade of inflammation (A0-1/2-3)	46/28	15/7	NS
Stage of fibrosis (F0-2/3-4)	64/10	21/1	NS
White blood cells (/μl)[b]	5,318 ± 1,617	4,489 ± 1,540	**0.032**
Neutrophils (/μl)[b]	2,913 ± 1,139	2,278 ± 983	**0.021**
Hemoglobin (g/dl)[b]	14.2 ± 1.4	14.1 ± 1.1	NS
Platelet count (×10^{-3}/μl)[b]	193 ± 105	171 ± 54	NS
ALT (IU/ml)[b]	79 ± 73	94 ± 92	NS
Pretreatment Serum HCV-RNA level (log(IU/ml))[a,c]	6.1 (3.6–7.4)	6.3 (4.0–6.7)	NS
PEG-IFN adherence (≧80%/<80%)	75/23	21/10	NS
RBV adherence (≧80%/<80%)	61/37	12/19	**0.024**
RVR/non-RVR	57/24	11/20	**0.001**

SNPs, single nucleotide polymorphisms; ALT, alanine transaminase; RVR, rapid virological response.
[a]Data are show as median (range) values.
[b]Data are expressed as mean ± SD.
[c]Data are shown as log (IU/ml)).
Bold indicated *P*-value of less than 0.05.

TABLE V. Multivariate Analysis for the Clinical and Virological Factors Related to Sustained Response With Peg-IFN Plus RBV Therapy in 63 Patients

Factor	Category	Odds ratio (95% CI)	*P*-value
Regression analysis			
RVR	RVR	1	**0.019**
	Non-RVR	0.170 (0.039–0.744)	
RBV adherence	≧80%	1	0.061
	<80%	0.250 (0.059–1.064)	
IL28B SNPs (rs8099917)	TT	1	0.104
	TG + GG	0.252 (0.048–1.330)	
Age		1.087 (0.976–1.211)	0.128
Neutrophils		0.999 (0.997–1.001)	0.209
White blood cells		1.000 (0.999–1.002)	0.504

CI, confidence interval; SNPs, single nucleotide polymorphisms; RVR, rapid virological response, RBV, ribavirin.
Bold indicated *P*-value of less than 0.05.

IL28B minor allele infected with both genotype 2a and 2b, and these differences were more profound in patients infected with genotype 2b than with genotype 2a. The rapid and sustained virological response rates of patients with the major IL28B allele were higher significantly than those of patients with the minor IL28B allele infected only with genotype 2b (rapid virological response: 58% and 0% with IL28B major and hetero/minor, $P = 0.002$, sustained virological response: 88% and 44% with IL28B major and hetero/minor, $P = 0.009$).

Although the rapid virological response rate of patients infected with genotype 2b was lower significantly than that of patients infected with genotype 2a, the sustained virological response rate was higher in patients infected with genotype 2b than with genotype 2a (Table II), In order to investigate that discrepancy, sustained virological response rates in patients with or without rapid virological response were analyzed according to IL28B SNPs. In patients infected with genotype 2b and a non-rapid virological response, the sustained virological response rates differed significantly between IL28B major and hetero/minor groups (sustained virological response with non-rapid virological response: 75% and 29% with IL28B major and hetero/minor, $P = 0.044$), and no one achieved a rapid virological response among the patients infected with genotype 2b and with the IL28B hetero/minor allele. In patients infected with genotype 2a, on the contrary, there was no significant correlation of rapid and sustained virological response rates between IL28B SNPs (sustained virological response with rapid virological response: 78% and 70% with IL28B major and hetero/minor, $P = 0.630$, sustained virological response with non-rapid virological response: 57% and 43% with IL28B major and hetero/minor, $P = 0.552$).

Next, changes in virological response rates over time were investigated in patients treated with PEG-IFN plus RBV and the time course was analyzed after separating the patients infected with genotype 2a and 2b (Fig. 1). Patients with IL28B-TG and -GG showed significantly lower rates of rapid and sustained virological response, compared to patients with IL28B-TT, and greater differences were observed according to IL28B SNPs among patients infected with genotype 2b than with 2a.

Side Effects

Side effects leading to Peg-IFN plus RBV discontinuation occurred in eight patients (6.2%) and discontinuation of RBV alone occurred in four patients (3.1%).

TABLE VI. Rapid and Sustained Virological Response Rates to Treatment According to IL28B SNPs

Character	IL28B major	IL28B hetero/minor	*P*-value
Number/total number (%)			
Overall			
RVR	58/88 (66)	10/24 (42)	0.031
SVR	81/100 (81)	17/29 (59)	0.013
Genotype 2a			
RVR	36/50 (72)	10/17 (59)	NS
SVR	43/57 (75)	13/20 (65)	NS
Genotype 2b			
RVR	22/38 (58)	0/7 (0)	0.002
SVR	38/43 (88)	4/9 (44)	0.009

RVR, rapid virological response; ETR, end of treatment response; SVR, sustained virological response.